Journal of Oceanology and Limnology
Vol. 40 No. 2, P. 530-550, 2022
https://doi.org/10.1007/s00343-021-1010-4

Methane in the Yellow Sea and East China Sea: dynamics, distribution, and production*

Wangwang YE[1, 2, 3, #], Guanxiang DU[1, 3, #], Honghai ZHANG[1, 3], Guiling ZHANG[1, 3, **]

[1] *Frontiers Science Center for Deep Ocean Multispheres and Earth System, and Key Laboratory of Marine Chemistry Theory and Technology, Ministry of Education, Ocean University of China, Qingdao 266100, China*

[2] *Key Laboratory of Global Change and Marine-Atmospheric Chemistry, Third Institute of Oceanography, Ministry of Natural Resources, Xiamen 361005, China*

[3] *Laboratory for Marine Ecology and Environmental Science, Pilot National Laboratory for Marine Science and Technology (Qingdao), Qingdao 266237, China*

Received Jan. 7, 2021; accepted in principle Feb. 26, 2021; accepted for publication Apr. 12, 2021

Abstract The Yellow Sea (YS) and East China Sea (ECS) are important marginal seas of the western Pacific. Understanding the dynamics of methane (CH_4) in the YS and ECS are essential to evaluate the role of coastal seas in global warming. We measured dissolved CH_4 at various depths in the water column of the YS and ECS during a cruise from March to April 2017. The concentrations of CH_4 varied greatly in different water masses, suggesting that the hydrographic conditions can substantially affect the CH_4 distribution. The CH_4 budget in the shelf of the ECS, which was estimated with a box model, suggests CH_4 consumption in the water column was the major sink (>95%), followed by a loss with a total of 2.2% CH_4 released to the atmosphere. Overall a local CH_4 production of 0.28 nmol/(L·d) was needed to maintain the CH_4 excess. Results from laboratory incubations showed an increase in CH_4 (1.5 times higher than the value of the control) after the addition of dimethylsulfoniopropionate (DMSP). Field incubations result in a CH_4 production rate of 1.2 nmol/(L·d) under a N-stressed conditions (N:P<1), indicates that the DMSP-dependent CH_4 production prefer to occur in the oligotrophic seawaters, where nitrogen is depleted. This study demonstrates that the marginal seas of China is a hotspot for CH_4 dynamics, and the cycling of methylated sulfur compounds (such as DMSP) may contribute importantly to locally formed CH_4. This may have further implication to carbon and sulfur biogeochemical cycles in the western Pacific.

Keyword: methane; East China Sea; Yellow Sea; aerobic production; dimethylsulfide (DMS); dimethylsulfoniopropionate (DMSP)

1 INTRODUCTION

Methane (CH_4) is an important greenhouse gas that influences the global climate (IPCC, 2013). Emissions of individual sources have been poorly quantified, even though the total global emissions of CH_4 into the atmosphere have been reasonably constrained (Saunois et al., 2020). Oceans cover 71% of the planet's surface and are considered a minor source of atmospheric CH_4 (Saunois et al., 2020). The CH_4 concentrations in the surface water of most of the world's oceans are 5%–75% supersaturated with respect to atmospheric CH_4 (Karl et al., 2008; Damm et al., 2009), implying a local in-situ methane source. In particular, studies showed that near-shore environment contributes the largest but most uncertain diffusive flux of the oceanic CH_4, but comprise only 3% of ocean surface areas (Weber et al., 2019). This observation can be partially attributed to the high CH_4 production rates and fast ventilation of the shallow

* Supported by the Ministry of Science and Technology of China (No. 2016YFA0601302), the National Natural Science Foundation of China (Nos. 41776122, 42006040), the Taishan Scholars Program of Shandong Province (No. 201511014), and the Aoshan Talents Program of the Qingdao National Laboratory for Marine Science and Technology (No. 2015ASTP-OS08)
** Corresponding author: guilingzhang@ouc.edu.cn
# Wangwang YE and Guanxiang DU contributed equally to this work and should be regarded as co-first authors.

water column (Borges et al., 2018; Schmale et al., 2018), or CH_4 escape from localized gas seeps via bubbles (Sakai et al., 1990; Judd, 2004; Shakhova et al., 2014; Di et al., 2020).

The Yellow Sea (YS) and East China Sea (ECS) are marginal seas in the northwestern Pacific Ocean, with average water depths of 44 m and 350 m, respectively. The distribution of dissolved CH_4 in the YS and ECS exhibits great temporal and spatial variability, which has been well documented in previous studies (Zhang et al., 2004, 2008a, b; Yang et al., 2010; Ye et al., 2016; Sun et al., 2018). Although several studies have reported that the surface and subsurface layers is supersaturated with CH_4 with respect to the atmosphere (Zhang et al., 2004; Ye et al., 2016; Sun et al., 2018), the mechanisms are still unclear.

Physical processes can contribute to the CH_4 accumulation at the ocean surface, including lateral transport from the CH_4-rich sources (e.g. estuaries; Borges et al., 2018) or vertical diffusion from subsea CH_4-hotspots (e.g. gas hydrates, cold seeps, and pockmarks) (Judd, 2004; Shakhova et al., 2014; Di et al., 2020). In the ECS, CO_2-rich fluids with other residual gas (including CH_4) were observed to emerge from the sea floor in the hydrothermal field (Sakai et al., 1990), suggesting the gas hydrates can serve as potential source to the aqueous CH_4 (Luong et al., 2019). Biotic factors contributing to the excess CH_4 was generally attributed to local production by microorganisms in anoxic microniches (de Angelis and Lee, 1994; Karl and Tilbrook, 1994; Stawiarski et al., 2019; Wäge et al., 2020). A recent mechanism that was proposed for maintaining surface CH_4 excess is that CH_4 is released as a byproduct via the decomposition of methylated compounds, such as methylphosphonate (MPn) and dimethylsulfoniopropionate (DMSP), when heterotrophic bacteria compete for nutrients (Repeta et al., 2016; Teikari et al., 2018). Studies for MPn identified the gene content and expression and thus confirmed the possibility of a Carbon-Phosphorus pathway for CH_4 formation at the biological level (Metcalf et al., 2012; Martínez et al., 2013; Sosa et al., 2017, 2020). Alternatively, DMSP is mainly produced in the cells of phytoplankton and can be transferred to the ambient water by grazing or sloppy feeding, so the yield and metabolism ratio of DMSP might be important for CH_4 formation. Damm et al. (2008) reported CH_4 production in the Arctic sea that was associated with the metabolism of DMSP and its degradation products. However, evidence for the formation of CH_4 from DMSP remains ambiguous and is mainly based on occasional correlations between CH_4 and DMSP concentrations (Damm et al., 2008; Florez-Leiva et al., 2013; Zindler et al., 2013; Damm et al., 2015; Zhai et al., 2019). In addition, the cleavage of the Carbon-Sulfur bond pathway (DMSP-to-CH_4) for CH_4 production has been rarely reported in other marine regimes, such as the marginal seas of the Pacific.

In this study, we examine the excess CH_4 in the upper water column of the YS and ECS and combine hydrographic conditions to discuss the factors that may influence the CH_4 dynamics in oxygenated waters. Then, we develop a preliminary CH_4 budget using a box-model to quantify CH_4 sources and sinks in the shelf of the ECS and evaluate the contribution from local CH_4 production to maintenance of the water column's CH_4 inventory. Finally, in combination with the field observation, we conduct laboratory incubation experiments alongside field observations to provide evidence that DMSP can serve as a potential precursor of CH_4, probably via demethylation in the YS and ECS. Thus, the understanding of CH_4 dynamics in the YS and ECS was improved by providing new data, conducting incubation experiments, interpreting these data and comparing with previous results (Zhang et al., 2004; Ye et al., 2016; Sun et al., 2018).

2 MATERIAL AND METHOD

2.1 Research area

The YS is a semi-enclosed continental shelf sea and is connected to the ECS and the Bohai Sea. The boundary between the ECS and YS spans from the northern tip of the mouth of the Changjiang (Yangtze) River to Cheju Island (Fig.1a). In winter and early spring, strong northerly winds that accompany a surge of cold, dry continental air tend to vertically homogenize most of the YS (Su, 1998). The coastal current flows southward near the Shandong Peninsula in the north and along the 50-m isobath in the south (Fig.1a). Water exchange between the YS and ECS mainly occurs near this boundary. Thus, three dominant water masses exist in the YS in spring, namely, the coastal water (CW) in the west, YS Central Water (YSCW) in the central trough, and YS-ECS Mixed Water (YEMW) near the boundary (Li, 1989; Su, 1998; Guan and Fang, 2006).

In spring, the western YS is mainly influenced by

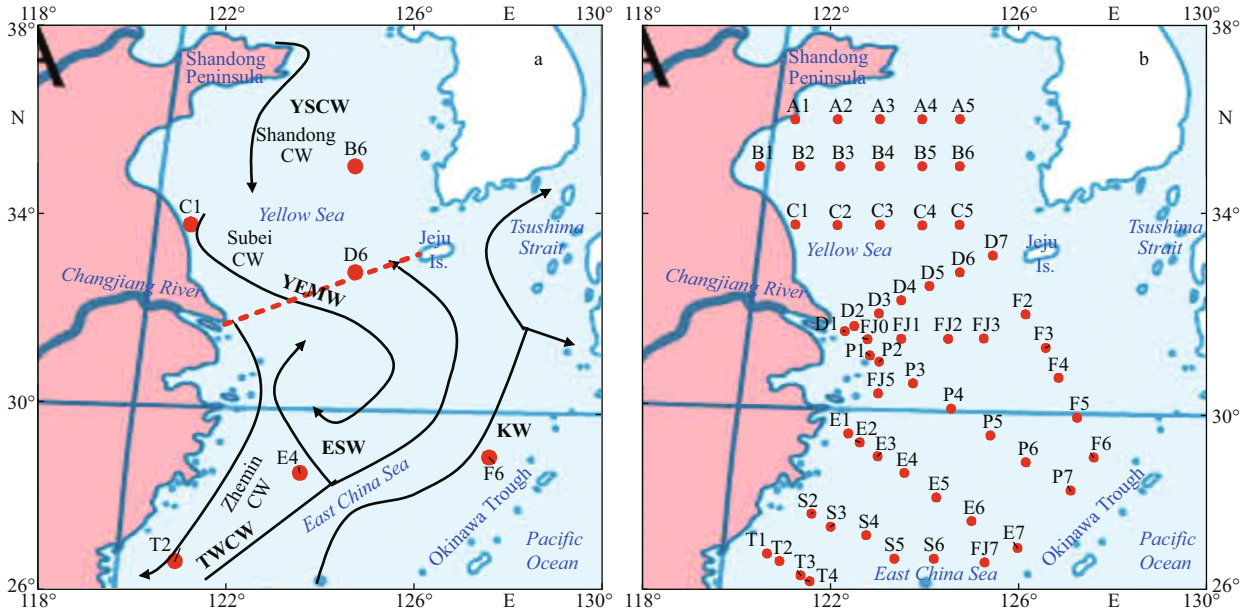

Fig.1 Schematic diagram of the circulation pattern in spring

a. water circulation modified from Guan and Fang (2006) and Yang et al. (2018); b. sampling locations in the Yellow Sea and East China Sea from March to April 2017. The six representative stations discussed in this study are shown in (a). The red-dashed line marks the boundary of the YS and ECS. The base map is derived from the Ministry of Natural Resources of China (No. GS(2020)4388). CW: Coastal Water; YEMW: YS-ECS Mixed Water; YSCW: YS Central Water; TWCW: Taiwan Warm Current Water; ESW: ECS Shelf Water; KW: Kuroshio Water.

the Coastal Water, which is fresh (salinity <32.0) and nutrient poor (nitrate <1.0 μmol/L) (Jin et al., 2013). The coastal water contains two components in the YS: Shandong coastal water forms around the Shandong Peninsula and flows southward along the 40–50-m isobaths, while the Subei CW lies in the southern, coastal regions, flowing southeast to the ECS and merging with remnants of Changjiang diluted water (Hickox et al., 2000). The YSCW is one of the main water masses that exist in the central YS throughout the year. This water displays great seasonal differences in salinity (31.0–32.0) and temperature (5.0–25.0 °C) because of seasonal stratification (Su, 1998). The YEMW is present in the southeastern YS, which consists of a branch of warm and saline water (from the ECS) that is mixed with YSCW. Thus, the YEMW exhibits high temperature (>9.0 °C) and salinity (>32.5) in spring.

In the ECS, the Changjiang River introduces freshwater from the west and flows southward in spring (Guan and Fang, 2006). From the east, the Kuroshio introduces water of high temperature and salinity, flowing northeast along the edge of the ECS and eventually turning east to the Korea Strait and Japan Sea (Fig.1a) (Tang, 1997; Li et al., 2012; Qi et al., 2014). Water exchange between the ECS and Kuroshio occurs across the shelf break through frontal processes at the surface and upwelling in the subsurface (Yang et al., 2018; Zhou et al., 2018). Importantly, this exchange introduces an intrusion of shelf water to the Kuroshio as turbidity tongue, increasing the exchanges in materials (such as nutrients and rare earth element) (Matsuno et al., 2009; Luong et al., 2018; Wang et al., 2019) and may affect the CH_4 concentrations at the Kuroshio subsurface (Luong et al., 2019). From the south, the Taiwan current flows to the north throughout the year between the 50- and 100-m isobaths (Su, 1998). In this study, we classified four dominant water masses in the ECS, namely, the coastal water (CW), ECS Shelf Water (ESW), Taiwan Warm Current Water (TWCW), and Kuroshio Water (KW) (Qi et al., 2014). The Kuroshio Water is usually considered to consist of four water masses, namely, the Kuroshio Surface Water (KSW), Kuroshio Sub-Surface Water (KSSW), Kuroshio Intermediate Water (KIW), and Kuroshio Deep Water (KDW) (Su, 1998; Zhou et al., 2018). The coastal water in the YS and ECS can be divided into three components: the Shandong, the Subei, and the Zhe-Min CW (Fig.1a). For simplicity, we refer to these three water masses as coastal water in this study.

The Zhe-Min CW (Fig.1a) forms from the mixing of seawater with runoff from the Changjiang River, Minjiang River, and other rivers. From spring to summer, the coastal water expands eastward and retreats northward, becoming warmer and fresher

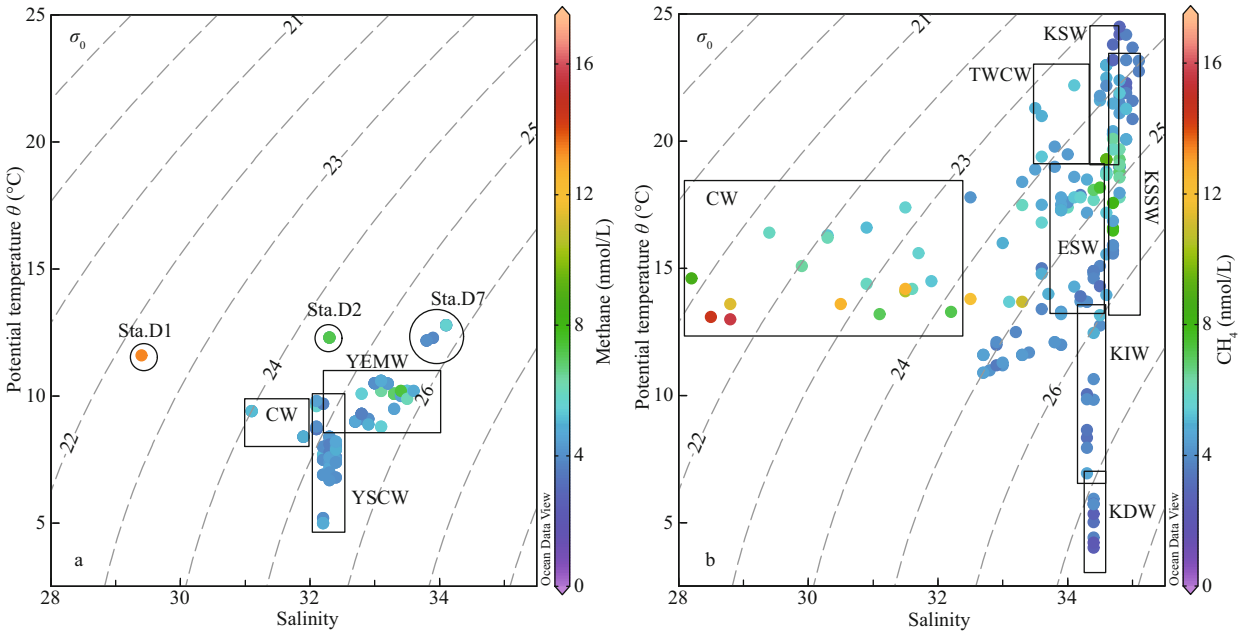

Fig.2 *T-S* diagrams and CH_4 concentrations (nmol/L) with isopycnic contours of the density (dashed lines, kg/m^3)

a. Yellow Sea; b. East China Sea. The classification of the water masses was based on Tang et al. (1997), Su (1998), Qi et al. (2014), Yang et al. (2018), and Zhou et al. (2018). CW: Coastal Water; YEMW: YS-ECS Mixed Water; YSCW: YS Central Water; TWCW: Taiwan Warm Current Water; ESW: ECS Shelf Water; KSW: Kuroshio Surface Water; KSSW: Kuroshio Sub-Surface Water; KIW: Kuroshio Intermediate Water; KDW: Kuroshio Deep Water.

(salinity <32.0; Fig.2b) (Qi et al., 2014). In contrast, the Kuroshio water on the outer shelf of the ECS showed relatively high temperature (>23.0 °C) and salinity (>34.2). The TWCW originates from the Taiwan Strait, bringing warm (>17.0 °C) and saline water (34.0–34.5) to the ECS (Yang et al., 2018; Zhou et al., 2018). This water runs northward along the 60-m isobath parallel to the coastal line and encounters the Subei CW in the eastern region off the Changjiang River (Fig.1a). The water mass in the middle continental shelf consisted of ECS water, TWCW, and a mix of KW and CW. These water masses have similar temperature-salinity (*T-S*) characteristics (Qi et al., 2014), so we collectively call them ESW.

2.2 Field sampling

In early spring of 2017, a cruise was conducted in the YS and ECS on the R/V *Dong Fang Hong 2* from 27 March to 11 April. A total of 57 stations along 10 lines were investigated during the cruise to obtain the overview distribution of biogenic gases in the study area (Fig.1b). Surface seawater for laboratory incubation experiments was collected from the coastal areas of the YS from November 2017 to March 2018. Seawaters for field incubation experiment were collected from the western North Pacific in a cruise during October 2018.

Water samples were collected at various depths by using 10-L Niskin bottles that were mounted on a rosette. At each station, we used Sea-Bird conductivity, temperature, and depth (CTD) probes (SBE 911 plus), which were equipped with ancillary sensors, to measure the salinity, temperature, and dissolved oxygen (DO) as functions of depth. Replicate samples for CH_4 analysis were obtained from the Niskin bottles in 100-mL glass vials by an overflow of approximately 1.5–2 times the bottle volume without bubbles. Afterwards, saturated mercuric chloride ($HgCl_2$) was added into the vials to inhibit microbial activity. Then, the vials were immediately sealed with poly tetra fluoroethylene (PTFE)/silicone septum and aluminum caps to avoid air contamination. Water samples for determining the dimethylsulfide (DMS) and DMSP concentrations were collected by using acid-cleaned polycarbonate bottles through silicone tubing that was attached to the Niskin bottles.

2.3 Box-model

The CH_4 budgets for the ECS shelf were evaluated by using a box-model, which was based on the concept of the conservation of water and salt masses (Chen and Wang, 1999; Zhang et al., 2007, 2018; Günthel et al., 2019). Briefly, we assume that the CH_4 inventory was temporarily constant in a specific water mass. Thus, the CH_4 concentration in these different water masses was the mean value of the stations that

Table 1 CH_4 concentration in water mass and the CH_4 rate used in box-model in the ECS

Type	Discharge ($\times10^6$ m^3/s)†	CH_4 concentration (nmol/L)	CH_4 saturation (%)	CH_4 rate (mol/s)#
Coastal water	0.01	10.9±3.8	401±132	0.11
Taiwan Warm Current Water	1.80	4.8±0.4	213±21	8.64
Kuroshio Surface Water	0.65	3.2±0.5	146±21	2.08
Kuroshio Sub-Surface Water	0.36	4.6±1.1	194±44	1.66
YS-ECS mixed water	0.01	5.3±1.1	182±36	0.05
ECS shelf water	-2.83	4.8±0.5	194±24	-13.58
Sea-to-air	–	–	–	19.41
Sediment-to-water	–	–	–	8.19
Oxidation	–	–	–	868.75
Production	–	–	–	881.01

†: the water-flux data are obtained from Zhang et al. (2007); #: the flux outflowing from the ECS is the balance of other water masses plus precipitation (6.2×10^3 m^3/s) and minus evaporation (1.0×10^4 m^3/s). Positive values indicate inflow and negative values indicate outflow; –: data not available or irrelevant.

belonged to these distinct water masses (classified by the salinity and temperature, Fig.2). Hence, the CH_4 fluxes (F_i, mol/s) during water transport could be obtained simply by the water flux (Q_i, m^3/s) times the CH_4 reservoir (C_i, nmol/L) in a specific water mass: $\sum Q_i \times C_i = F_i$. Then the CH_4 mass balance in the ECS shelf can be expressed as: $\sum F_i + R_{air} + R_{sed} + R_{con} + R_{pro} = 0$, where F_i represents the water-transported CH_4 input (+) and outflow (–) over the shelf (Table 1), R (mol/s) indicates the rates of CH_4 accumulation (+)/elimination (–), including sea-to-air exchange (R_{air}), sedimentary release (R_{sed}), microbial consumption (R_{con}), and production (R_{pro}). The R_{air} and R_{sed} were computed by the interface-fluxes (μmol/(m^2·d)) times the shelf area (~5.1×10^5 km^2) as indicated by Ye et al. (2019). The R_{con} was calculated by the shelf water volume (~2.7×10^{14} m^3) multiplies the CH_4 oxidation rate (OR, nmol/(L·d)). The OR was calculated using a first-order equation ($OR = k \times C_{ESW}$) as reported by Rogener et al. (2018, 2019), where k is the turnover rate constant and C_{ESW} is the mean CH_4 concentration in the ESW (Table 1). The net production rate (R_{pro}) was the balance of other sources and sinks.

2.4 Incubation experiment

Four separate incubation experiments were conducted to study the links between DMSP/DMS degradation and CH_4 production. The laboratory experiments were conducted at the Ocean University of China (Qingdao) and the field incubation experiment was conducted onboard. The seawater for these experiments was placed into an acid-cleaned polycarbonate carboy before the start of the experiment. For the first experiment, a final concentration of 100-μmol/L DMSP was directly added into the carboy. After mixing homogeneously, the seawater in the carboy was transferred into 160-mL glass bottles as the DMSP-amended group. Subsamples were dispensed into the glass bottles prior to the addition of DMSP as the control treatment. This experiment was conducted in November 2017 and repeated in January 2018. The second incubation experiment was set to identify the effect of nutrient-stressed conditions (in particular, N deficiency) on DMSP-dependent CH_4 production. Specifically, the carboy was amended with phosphate (P) to a final concentration of 10.0-μmol/L. Subsamples were dispensed into the glass bottles as the control treatment. Afterwards, DMSP was added to the carboy to a final concentration of 1.0 mmol/L, and then the water was placed into another group of glass bottles as the (P+DMSP) treatment (N:P<1, N-depleted). Finally, additional subsamples were collected after the carboy was sequentially amended with 50.0-μmol/L and 160.0-μmol/L nitrate, which were the (P+DMSP+N) treatments (5<N:P<16, N-stressed or N-rich). The third incubation experiment was implemented to test the direct effect of spiked DMS on CH_4 production. Similarly, subsamples were sequentially transferred from a carboy that was amended with different nutrients, including glucose (100.0-μmol/L C), nitrate (16.0-μmol/L N), phosphate (1.0-μmol/L P), and DMS (100.0 mmol/L). Then, the bottles were assigned to the control (without addition), the (C+N+P) treatment, and the (C+N+P+DMS) treatment. The fourth incubation was conducted in the western North Pacific to test the DMSP-dependent CH_4 production in the oligotrophic areas (station E24, 130°E/5°N, see detail in Ye et al. (2020)). The DMSP (final concentration of 10.0 μmol/L) was amended

directly into the surface waters without any other additions, which was the DMSP treatment. Natural seawaters incubated under the same conditions then assigned to the control. All the bottles were filled with 150-mL seawater and 10-mL headspace volume (except for the fourth experiment with 50-mL seawater and 10-mL headspace volume), sealed with PTFE/silicone septum, crimped with aluminum caps, and incubated in a 12-h:12-h light-dark cycle incubator or in the onboard-surface-water-circulation-system that was maintained at nearly in-situ temperatures (~25 °C). At each time point per day, triplicate bottles per treatment were randomly sacrificed to obtain the CH_4 and DO concentrations. The DO was measured by using the Winkler titration method (Bryan et al., 1976).

2.5 Chemical analyses

CH_4 was determined by the headspace method for the incubation samples (Bange et al., 2010) or the gas-stripping method for the field samples (Zhang et al., 2004). The CH_4 in the headspace was measured by a Shimadzu GC-14B gas chromatograph that was packed with Porapak Q (80–100 mesh) and fitted with a flame ionization detector (FID). The CH_4 was quantified by calibrating peak areas to the FID's response to a three-point calibration by using known-volume injections of CH_4 standards (CH_4:N_2 mixtures of 2.0×10^{-6}, 4.0×10^{-6}, and 50.0×10^{-6}, China Institute of Metrology). For the field samples, seawater was introduced into a stripping chamber and purged with high-purity nitrogen. After bubbling, the dissolved CH_4 was passed through a desiccant tube to remove water vapor. The CH_4 was concentrated onto a stainless steel trap that was filled with 80–100 mesh Porapak Q and then was released into a Shimadzu GC-14B gas chromatograph for separation and quantification (Zhang et al., 2004).

A purge-and-trap system was used to analyze the DMS concentration, as previously described by Yang et al. (2008). Dissolved DMSP ($DMSP_d$) was determined by using the small-volume drip filtration method by Li et al. (2016). Briefly, a known volume of seawater was gently filtered by a Whatman GF/F glass fiber filter (0.7 μm). The DMSP in the filtrate was then converted completely to DMS by adding sodium hydroxide (5-mol/L NaOH), and the generated DMS was analyzed by the same technique. The total DMSP ($DMSP_t$) concentrations were directly analyzed from unfiltered alkaline subsamples. The concentrations of particulate DMSP ($DMSP_p$) were calculated by subtracting $DMSP_d$ from the $DMSP_t$ value (Li et al., 2016).

The seawater for chlorophyll *a* (chl *a*) analysis was first filtered through a 0.45-μm pore-size filter (Whatman GF/F). Then, the chl *a* was extracted by soaking in 90% acetone and measured by using a fluorescence spectrophotometer (Turner Designs, USA) (Zhai et al., 2019).

2.6 Statistical analysis

Principal component analysis (PCA) is a multivariate statistical analysis technique, in which a group of correlated variables is transformed into a new group of variables that are uncorrelated or orthogonal to each other (Jackson, 1991). The datasets of the field cruise were analyzed by using PCA and the correlation matrix. Prior to the statistical analysis, the variables were standardized to eliminate the influence of differences in the data magnitude and measurement scales (Webster, 2009). A VARIMAX rotation was performed to aid with the interpretation of the results. Factors with eigenvalues of 1.0 or greater were selected and considered significant. Factor loading (FL) is defined as the correlation coefficient between the principal component score and each variable (Yamamoto et al., 2014). Additionally, univariate analysis of variance (ANOVA) was used to determine whether the CH_4 concentrations and production rates varied between treatments with or without the addition of DMS/DMSP. The homogeneity of the variance was checked by using Levene's test prior to the ANOVA. Differences were considered statistically significant when P was less than 0.05.

3 RESULT AND DISCUSSION

3.1 CH_4 in different water masses in the YS and ECS

The main water masses that existed in the YS during March 2017 were classified in the *T*-*S* plot to constrain the CH_4 biogeochemical processes (Fig.2a). The CH_4 concentrations varied greatly within the different water masses in the shallow YS, ranging from near atmospheric equilibrium (3.3 nmol/L, 107%) in the YSCW to a mean value of 4.8±1.1 nmol/L in the coastal water and a peak value of 6.9 nmol/L (241%) in the YEMW (Table 1). This distribution resulted in a north-south concentration gradient on the shelf because the concentrations tended to increase towards the south of the YS. Indeed, the highest CH_4

concentration (14.8 nmol/L) was observed in the southern YS at station D1 (Fig.1b). This high value could be attributed to the CH_4-rich Changjiang diluted water with low salinity (25.8) and density (<23.5 kg/m^3). Consequently, the CH_4 concentration at station D2 (mean:6.1±1.5 nmol/L) was the result of mixing with diluted water and Coastal Water, corresponding to relatively high salinity (32.3) and density (24.4 kg/m^3). The surface water of the Changjiang River was reported to contain high CH_4 (e.g., >100.0 nmol/L) (Zhang et al., 2008a; Ye et al., 2016; Sun et al., 2018). Thus, mixing between diluted water and the coastal water near the boundary of the YS could have partially contributed to the north-south CH_4 gradient. In contrast, lower CH_4 concentrations (mean: 3.9±0.2 nmol/L) were observed in the northern central regime, as influenced by YSCW (such as stations A3 and A4; Fig.1b). Station D7 was located in the western area off Jeju Island. Although this area belongs to the YS in this study, the dominant water mass at this station was ECS Water according to the *T-S* characteristics (temperature: 12.2–12.8 °C, salinity: 33.8–34.1, density: 25.5–25.8 kg/m^3; Fig.2a & b), which implies the exchange of YS and ECS water near the boundary.

The CH_4 varied greatly in the different water masses across the shelf of the ECS (Fig.2b), ranging from undersaturation (2.2 nmol/L, 66%) to significant oversaturation (15.7 nmol/L, 566%) with respect to the atmosphere. In the shallow coastal areas (depth <50 m) and middle continental shelf (depths of 50–100 m), the CH_4 concentrations generally decreased with increasing longitude, ranging from an average of 10.9±3.8 nmol/L in the CW to 4.8±0.5 nmol/L in the ESW and 4.8±0.4 nmol/L in the TWCW (Table 1). The rapid CH_4 decrease in the ESW compared to the CW was likely the result of microbial CH_4 oxidation in the water column and emission into the atmosphere (Zhang et al., 2008b; Ye et al., 2016; Sun et al., 2018). At stations with water depths greater than 100 m, the CH_4 concentrations were typically less than or near equilibrium to the atmosphere. These areas were essentially influenced by the Kuroshio (Fig.1b), and the low measured CH_4 concentrations in the KIW (mean: 3.9±0.4 nmol/L) and KDW (3.2±0.7 nmol/L) indicated that CH_4 had been consumed in the water column. An exception occurred at water depths of 200–300 m, where CH_4 peaks (4.8–8.2 nmol/L) were observed. No other source (such as lateral transport or vertical diffusion) was present in the Kuroshio-influenced area (Zhang et al., 2004), so we speculate that these maxima were correlated with in-situ CH_4 production, which will be discussed in the following sections. Thus, the CH_4 concentrations were believed to be associated with different water masses (e.g., the CH_4 in the coastal water was more than two times higher than the CH_4 in the Kuroshio). However, the vertical CH_4 distribution showed great spatial variations, and the water masses could only generally explain the CH_4 sources in the YS and ECS.

3.2 Vertical distribution of dissolved CH_4 in the YS and ECS

The depth profiles of hydrographic features and CH_4 concentrations varied greatly in the entire study area, and they could be classified into different sub-groups according to the dominant water masses. We found that stations in the same group had similar features in the vertical profiles. Thus, the depth profiles at six representative stations were chosen to show the spatial variability of CCW, YSCW, and YEMW, while stations T2, E4, and F6 in the ECS were dominated by TWCW, ESW, and KW (Fig.1b).

Station C1, which had low salinity (31.1) and temperature (9.4 °C), is located in the western YS, where the coastal water is the dominant water mass. The average water depth was quite shallow (16 m), and the physical parameters were well mixed from the surface to the bottom in early spring (Fig.3a). Because of this strong vertical mixing, the dissolved CH_4 barely varied in the water column, ranging from 5.2 nmol/L at the surface to 5.0 nmol/L at the bottom. The water is oversaturated in CH_4 with respect to the atmospheric equilibrium, implies that CH_4 can be significantly released from the water column to the atmosphere. Station B6 is located in the central trough of the YS, where YSCW was the dominant water mass during the investigated period (Fig.3b). The overall CH_4 concentration at station B6 (mean value of 4.4±0.2 nmol/L) was lower than that at station C1 (mean value of 5.1±0.1 nmol/L); as indicated previously, the CH_4 had lower concentrations in the YSCW than in the CW (Fig.2a). The input of fresh water (i.e., Sheyang River) near the coast can explain the CH_4 difference between the coastal area (CW) and the central YS (YSCW). However, the CH_4 concentrations at both stations were 1.5–1.8 times higher than the atmospheric equilibrium and were also higher than the reported values from previous studies for the same season (Zhang et al., 2004). The excess CH_4 in the well-mixed water could have been released into the

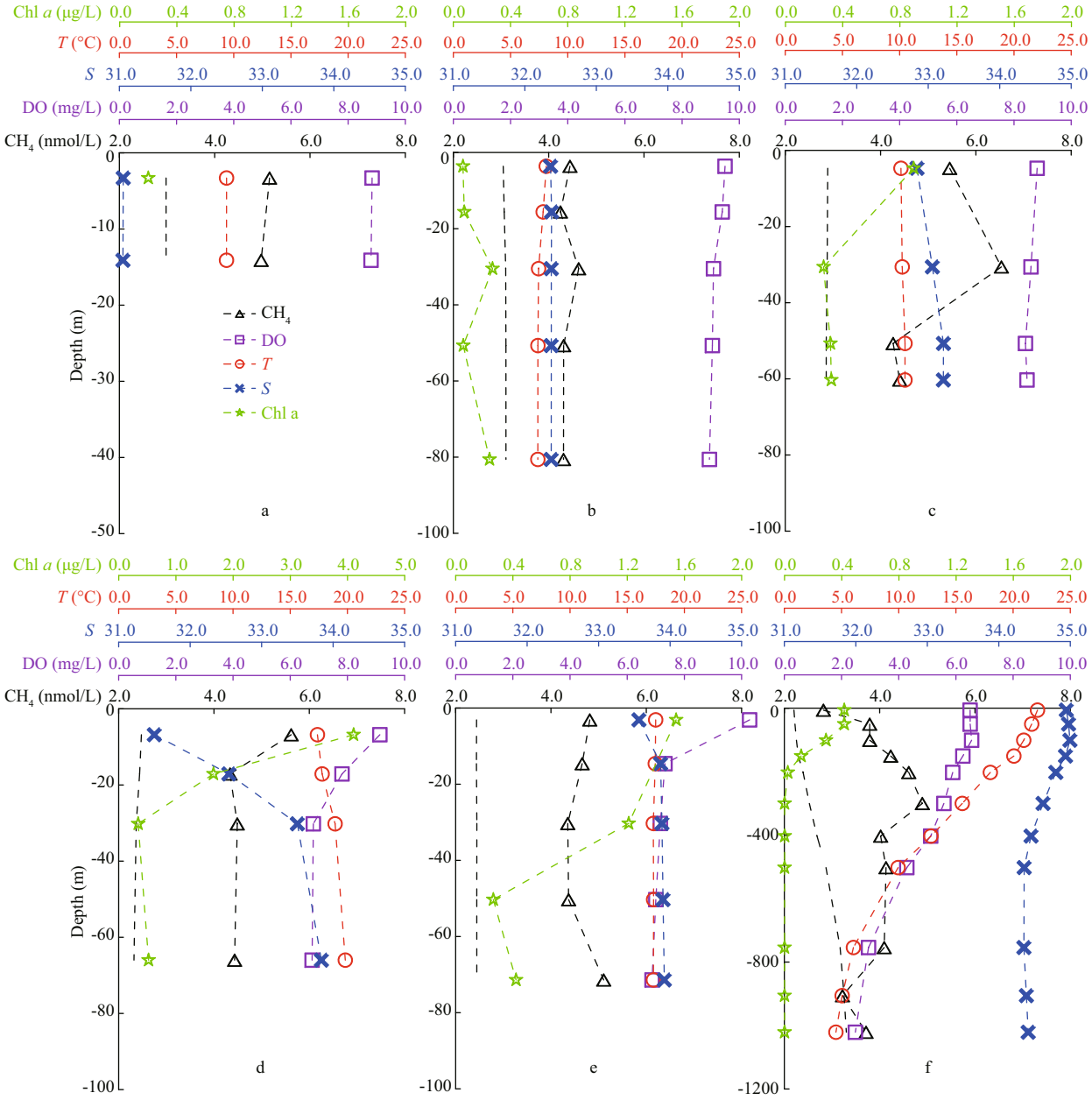

Fig.3 Vertical profiles for the temperature (°C), salinity, DO (mg/L), chl *a* (μg/L), and CH_4 (nmol/L) at six representative stations in the YS (a–c) and ECS (d–f)

a. station C1; b. station B6; c. station D6; d. station T2; e. station E4; f. station F6.

atmosphere, with a mean rate of 1.3 μmol/(m^2·d) (Zhang et al., 2004). Thus, additional CH_4 sources should have existed to sustain a stable value of CH_4 (such as 4.4 nmol/L at station B6) in the water column. Sediment release did not appear to be an important source for the water column's CH_4 in the YS and barely contributed to the atmospheric CH_4 because of the low organic-carbon concentrations (~0.3%) in the sediment and the presence of abundant DO (>9.0 mg/L) in the bottom water (Zhao et al., 2018). Moreover, only 5.4% of the sedimentary organic carbon was degraded in the YS sediments, which was three times lower than that in the ECS (Zhao et al., 2018). The low remineralization rates of organic carbon restrict the upward flux of CH_4 in sediments (Valentine, 2002). Consequently, limited CH_4 could diffuse through the sediment-water interface in the YS because of anaerobic/aerobic CH_4 oxidation (Jørgensen et al., 2001; Treude et al., 2005). In addition, CH_4-rich CW could not be transported to the central YS (such as station B6), so the extra CH_4 source should have been attributed to

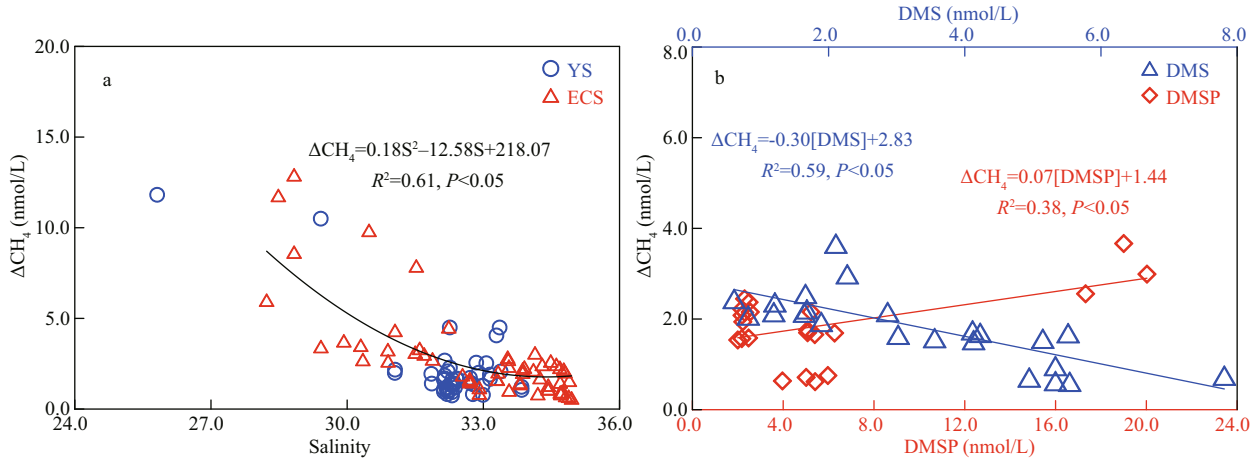

Fig.4 Correlations between ΔCH$_4$ (nmol/L) and other parameters

a. salinity vs. ΔCH$_4$. Blue circles and red triangles represent data constrained in the YS and the ECS at depth below 20 m. Black line showed the best fit of the total data; b. DMS (blue triangles)/DMSP (red diamonds) vs. ΔCH$_4$. Date were constrained from those offshore stations (water depth >800 m) within the water column of 0–300 m.

in-situ CH_4 production and our incubation experiments suggested that DMSP may have been a potential substrate for CH_4 production in the study area (see details in Section 3.4).

At station D6 which is the boundary of ECS and YS (Fig.3c), the surface layers were influenced by the YEMW, but the bottom layer was likely a component of the ECS water. CH_4 concentrations increased from 5.5 nmol/L at the surface to 6.5 nmol/L at a depth of 30 m and then dropped to 4.3 nmol/L at the bottom. Thus, the high CH_4 concentrations (>5.0 nmol/L) in the upper 30 m were the result of mixing, while the relatively low values (<5.0 nmol/L) below this layer were characteristic of ECS water, further indicating the influence of the water masses on the CH_4 distribution.

Significant correlations between excess CH_4 (ΔCH_4, $C_{\text{in-situ}}$–$C_{\text{equilibrium}}$) and salinity (P<0.05, Fig.4a) were found in the water columns both in the YS and ECS, suggesting that the mixing with fresh water has important effect on CH_4 distribution in the nearshore regions. In the ECS, however, more complex hydrography influences CH_4 distribution. For example, at station T2 near the coast (Fig.3d), the water layer of the surface 30 m was influenced by the coastal water and while water below 30 m could be attributed to the TWCW (Li et al., 2012). Consequently, the chl-*a* concentration dropped to <0.5 μg/L below 30 m, and the CH_4 concentration was higher in the surface layer (5.6 nmol/L) than in the bottom layer (4.4 nmol/L). Hence, we carefully chose stations that could represent the properties of different water masses to calculate the CH_4 inventories in these waters, and the mean value of CH_4 in the TWCW was 56% of the mean value in the CW (Table 1). However, the CH_4 concentrations in the water masses in the ECS exhibited seasonal variations. For example, our observed CH_4 in the TWCW in early spring was 21% lower than what was reported for summer (Zhang et al., 2008b).

Station E4, which is located in the middle of the continental shelf, had a well-mixed water column below a depth of 15 m (Fig.3e). The CH_4 only decreased by 0.4 nmol/L within the top 50 m and then reached a maximum of 5.1 nmol/L in the bottom water, suggesting a possible CH_4 source from sediments. Previous studies showed that the sedimentary release of CH_4 in the ECS is an important source of dissolved CH_4 in the water column, and the release rates from the sediment to the water column varied 0.6–2.3 μmol/(m^2·d) in season (Zhang et al., 2008a; Sun et al., 2018). Thus, the sediment-water CH_4 flux was ~10% of the sea-air CH_4 flux (Sun et al., 2018), indicating that sediment was a potential source of the dissolved CH_4 in the ECS. Our results showed that the CH_4 in the ESW was comparable to that in the TWCW (Table 1), matching the summer observations by Zhang et al. (2008b).

Station F6 is located at the edge of the Okinawa Trough, where the mainstream of Kuroshio flows northeastward and intrudes the ECS along the continental slope (Figs.1a & 3f). Thus, the main features of the Kuroshio can be captured from this station. Specifically, the high temperature (22.1 °C) and salinity (34.8) in the surface layer indicate the existence of KSW. The maximum and minimum salinity at depths of ~150 and ~500 m showed the characteristics of KSSW and KIW, respectively. In

addition, the low temperature (<6.0 °C) and high density (>27.0 kg/m^3) at depths below 700 m showed the features of KDW. Consequently, the CH_4 increased in the subsurface layer (50–300 m) and reached a maximum of 4.9 nmol/L. This value subsequently decreased between depths of 300 and 800 m and fluctuated around the atmospheric equilibrium in deep water (800–1 000 m). This CH_4 profile showed the characteristics of the Kuroshio, with relatively rich CH_4 occurring in the KSSW (4.6±1.1 nmol/L) and KIW (3.9±0.4 nmol/L) and poor CH_4 occurring in the KSW (3.2±0.5 nmol/L) and KDW (3.2±0.7 nmol/L). The CH_4 in the KSSW was comparable to that in the ESW, probably resulting from an intrusion of shelf water as a turbidity tongue (Luong et al., 2018, 2019). In contrast, CH_4 in the KSW and KDW were 33% and 71% lower than that in the ESW and CW, respectively (Table 1). Compared to previous studies, the observed CH_4 in the KSW in this study was 1.1–1.4 times higher than that in the spring and summer (Zhang et al., 2004, 2008b), but 20% lower than that in the autumn (Sun et al., 2018). The temperature may be a driver of CH_4 variations in the KSW during different seasons (Sun et al., 2018). Meanwhile, the upward diffusion of CH_4 in the subsurface layer may be another factor that determines the magnitude of surface CH_4. Subsurface CH_4 maxima at depths between 200 and 300 m were observed at the deep stations (>800 m, stations P7, FJ7, E7, and F6). Consequently, CH_4 gradients existed within the top 200–300 m, with the intensity ranging from 0.006 nmol/(L·m) to 0.026 nmol/(L·m). The presence of these gradients implies that excess CH_4 formed locally in the subsurface water, subsequently diffused to the surface, and eventually entered the atmosphere.

3.3 CH_4 budget in the shelf of the ECS

The ECS shelf is likely a transition zone between the coast and open ocean. The exchanging of water masses, heat, nutrients, and other materials occur on this shelf, which has far-reaching effects on the northern Pacific (Jiang et al., 2018). Understanding the CH_4 dynamics in the shelf water, therefore, is crucial for investigating the CH_4 biogeochemical processes in the ECS. In early spring, the Changjiang flows southward and becomes the coastal water by mixing with shelf water, whereas the Kuroshio flows northeastward along the edge of the ECS and intrudes the shelf mainly through the KSW and KSSW (more than 80%) (Su, 1998; Zhou et al., 2018). When

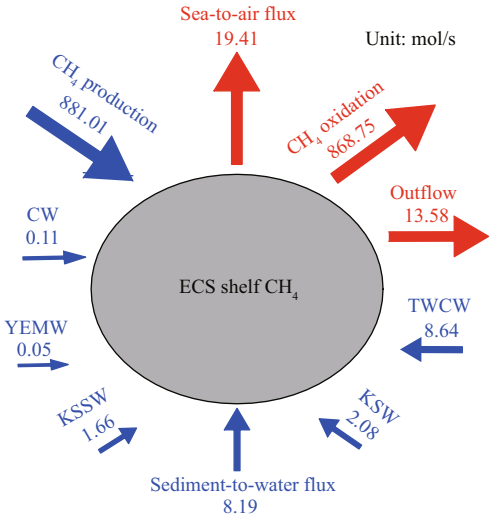

Fig.5 Preliminary CH_4 budget in the shelf of the ECS

The CH_4 fluxes in box-model calculations are provided in Table 1.

examining the water budgets of the ECS, the discharges of KSW and KSSW inflows into the shelf were two orders of magnitude higher than that of the coastal water (Table 1). However, the TWCW comprised ~64% of the total water inflow in spring, and the ECS received ~0.01×10^6 m^3/s influx from the YS. Consequently, the outflows through the Tsushima Strait and Japan Sea were estimated as 2.83×10^6 m^3/s. We estimated the CH_4 that was carried by the coastal water to be only 0.11 mol/s, which was 15–19 times lower than what was transported via the KSW and KSSW but comparable with the input through the YS (0.05 mol/s), suggesting that the influx of freshwater was a minor source (0.01%) of shelf CH_4 in early spring because of the low water discharge (Table 1; Fig.5). The gas hydrates located at the Okinawa Trough may play an important role in contribution of high CH_4 to the Kuroshio and the CH_4 concentrations venting from the hydrothermal field were recorded at millimole level (Sakai et al., 1990; Luong et al., 2019), raising the concerns of gas hydrates in contribution to the shelf CH_4. However, the fluids were diluted quickly and diffused northwest carried by the Kuroshio, resulting in a relatively low CH_4 inventory (2.2–5.3 nmol/L) (Luong et al., 2019) that matches with our observation at the KSSW (4.6±1.1 nmol/L, Table 1). This means the gas hydrates located at the Okinawa Trough (water depth>800 m) would have small impact on the CH_4 distribution in the ECS shelf (<200 m) due to diluting and consuming. The TWCW brought the most CH_4 to the shelf in spring (8.64 mol/s). Thus, the TWCW could be considered an important source of the shelf's CH_4 inventory. The total out-flux was 8% higher than

the total input, implying that the ECS shelf was a net CH_4 source to the open ocean. The differences between the total inflow and outflow also suggested the existence of other CH_4 sources in the ECS (e.g., in-situ production, groundwater, and sedimentary release). However, these CH_4 fluxes may exhibit seasonal variations. For example, Zhang et al. (2008b) reported that the net CH_4 out-flux from the shelf in summer was more than five times higher than our results in early spring. The difference in freshwater discharge, which was more than three times higher in summer than in winter (Zhang et al., 2007), was the main reason for these seasonal CH_4 changes. In addition, the net CH_4 outflow in this study was 56% of what was previously reported in the same season (Zhang et al., 2004). The estimation of the net out-flux in this previous study did not consider TWCW, which is believed to be an important CH_4 source according to our study. Thus, our data showed a reasonable CH_4 budget in the shelf.

The sedimentary release of CH_4 was proven a potential source of dissolved CH_4 in the ECS shelf (Fig.3e) (Zhang et al., 2008a; Sun et al., 2018). The quantity of CH_4 that was emitted from sediments showed great seasonal variations, presumably lower in winter and higher in summer, especially under hypoxia conditions off the Changjiang River estuary (Zhang et al., 2008a; Ye et al., 2016; Sun et al., 2018). The CH_4 fluxes from sediment to the water in the ECS were documented in previous studies, such as 0.8 μmol/(m^2·d) in April/May 2002 (Zhang et al., 2008a) and 1.7–2.2 μmol/(m^2·d) in March 2011 (Sun et al., 2018). We used the average of these studies to represent the mean sediment-water CH_4 flux in the ECS in spring since we did not measure the sediment-to-water flux in our study. Thus, the sediment-water CH_4 flux was estimated as 8.19 mol/s based on the shelf area. This result indicates that the sediment in the ECS was a comparable source to the TWCW for the shelf CH_4. From literatures, we found benthic CH_4 fluxes varied spatially. Fox example, in the Baltic Sea, the fluxes ranged from 100 μmol/(m^2·d) in coastal area to 26 000 μmol/(m^2·d) in the inner eutrophic estuary (Sawicka and Brüchert, 2017). Another study reported the CH_4 flux at the sediment-water interface was estimated 20.9–25.1 μmol/(m^2·d) in the Godavari and Krishna estuaries (Rao and Sarma, 2016). Our results were comparable with that reported in the west coast of India (4.71 μmol/(m^2·d)) (Araujo et al., 2018) and in the continental shelf of the Gulf of Cádiz (0.9–24 μmol/(m^2·d)) (Ferrón et al., 2009). With respect to the CH_4 emissions to the atmosphere, we used the mean value of 3.3 μmol/(m^2·d) that was calculated by Du et al. (unpublished data) for this cruise to represent the sea-air CH_4 flux in the ECS in spring. Thus, the sea-air CH_4 flux (19.41 mol/s) was one of the major CH_4 sinks in the ECS shelf and was more than ~1.5 times higher than what was transported by water masses, suggesting that the ECS is a net source of atmospheric CH_4. The CH_4 oxidation rate (OR) can be measured by radiotracer techniques using tritiated CH_4 according to the method described by Bussmann et al. (2017). Here, we used the turnover rate constant (k) in the North Sea, with a mean value of 0.058/d, reported by Osudar et al. (2015), to calculate the CH_4 oxidation rate in the ECS shelf in our study because the environmental conditions in the North Sea were similar to that in the ECS. Thus, the CH_4 oxidation rate was computed as 0.278 nmol/(L·d) when considering the mean CH_4 concentration of 4.8 nmol/L in the ECS shelf (Table 1). Meanwhile, a comparable CH_4 oxidation rate (0.265 nmol/(L·d)) was measured by a ^{13}C-tracking method deployed in this survey. The consistency of CH_4 oxidation rate from different methods indicates that the result we used in the CH_4 budget is reasonable. Consequently, the R_{con} in the shelf water was calculated as 868.75 mol/s by multiplying the shelf water volume by the CH_4 oxidation rate. Taken together, a CH_4 production rate of 881.01 mol/s was calculated after balance of other sources and sinks in spring (Fig.5). Considerable CH_4 should be produced in the water column to sustain the CH_4 deficit. According to the shelf water volume, our mass balance indicated that a local CH_4 production rate of 0.28 nmol/(L·d) was required to maintain the CH_4 loss. This value is in the range of the reported CH_4 production rates from Mexico Bay (-0.04–2.00 nmol/(L·d)) (Bange et al., 1994) but much lower than what was reported for oligotrophic lakes (~50.00 nmol/(L·d)) (Grossart et al., 2011). Hence, our results showed that local production/consumption is the major source/sink (>95%) of CH_4 in the ECS shelf, following by a total of 2.2% CH_4 diffused to the atmosphere. It should be noted that the estimation contains great uncertainties due to insufficient field data (e.g. gas fluxes at seep sites) and the source flux was presumably underestimated without consideration of the contribution of the gas hydrates. It is hard to quantify because rare data was published to constrain the size, area, and gas spreading velocity in various seeps. This means the local CH_4 production rate was

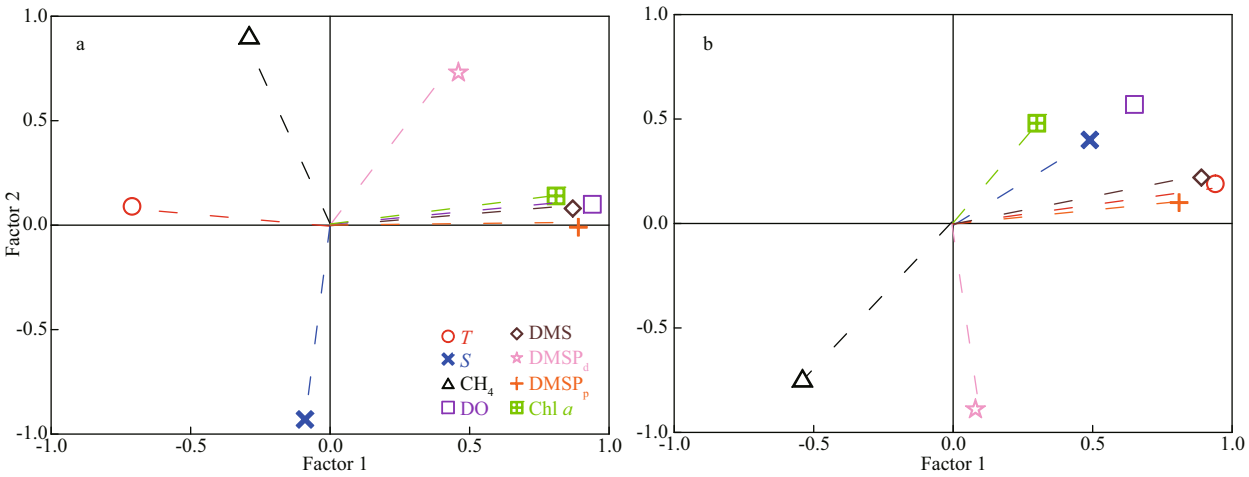

Fig.6 Loading plots that correspond to the first two factors following the VARIMAX rotation of the principal components

a. in the YS; b. in the ECS. Dataset from the ECS is derived from deep stations (>800 m).

overestimated to some extent but would not affect the fact that the ECS was a hotspot for CH_4 dynamics (production, consumption, and emission).

3.4 CH_4 formation via DMSP/DMS degradation

Field observations suggested the presence of excess CH_4 in the subsurface layers and the box model indicated the significant potential for CH_4 production in the study area. As DMSP has been recently suggested as the possible substrate for CH_4 production (Damm et al., 2015; Stawiarski et al., 2019), we measured the dissolved and particulate fractions ($DMSP_d$ and $DMSP_p$) (data not shown) in the field survey. No correlations between DMSP/DMS and CH_4 were found when all the stations in the ECS were considered. However, a negative correlation between DMS and ΔCH_4 (R^2=0.59, P<0.01) and positive correlation between $DMSP_d$ and ΔCH_4 (R^2=0.38, P<0.05) were found at offshore stations (water depth >800 m) within the water column of 0–300 m (Fig.4b). Further, to weaken the influence of multiple factors, the parameters at deep-water stations (>800 m, stations P7, FJ7, E7, and F6) were analyzed by using PCA to determine potential correlations between the Carbon-Sulfur bonded compounds and CH_4 distribution (Fig.6). Weak correlations between CH_4 and DMSP/DMS were found in the YS (Supplementary Tables S1–S2). In contrast, two factors were extracted in the ECS, explaining a cumulative variance in the data of 69% (Supplementary Tables S3–S4). Thus, the first factor was associated with the features of dissolved gases because the temperature (FL=0.94) and dissolved gas content (DO: FL=0.65, DMS: FL=0.89, CH_4: FL=-0.54) were strongly loaded (Fig.6b). The second factor, however, was significantly loaded by $DMSP_d$ (FL=-0.89), indicating that this factor was related to the cycling of methylated sulfur compounds. CH_4 (FL=-0.74) was strongly loaded in the second factor, suggesting correlations between CH_4 and $DMSP_d$. Thus, we speculate that $DMSP_d$ and its degradation product (DMS) may serve as CH_4 precursors in the study area, particularly in oligotrophic areas.

To assess this hypothesis, incubation experiments were conducted in the laboratory as well as in the field. In our first experiment, spiking treatments with $DMSP_d$ significantly increased the CH_4 concentration compared to the control groups (Fig.7a, ANOVA, P<0.01 and Fig.7c, ANOVA, P<0.05). The oxygen content in the glass bottles was constantly above 5.0 mg/L, illustrating the well-oxygenated conditions during the incubation period (Fig.7b & d). Thus, these results showed that the amendment with DMSP induced CH_4 production, and DMSP can act as a precursor for CH_4 formation in oxic water. Furthermore, different N:P ratios were set in the second experiment to test the effect of N deficiency on DMSP-dependent CH_4 production, as indicated by Damm et al. (2009). In particular, the addition of DMSP increased the CH_4 to ~15.0 nmol/L in less than a week, 1.5 times higher than the value of the control (Fig.8a). The DO in the control was almost constant during the entire incubation, whereas the DO in the DMSP treatments rapidly depleted over the first three days and gradually decreased to approximately 5.0 mg/L after seven days of incubation, suggesting strong respiration (Fig.8b). The effect of N deficiency on the microbial utilization of DMSP was ambiguous

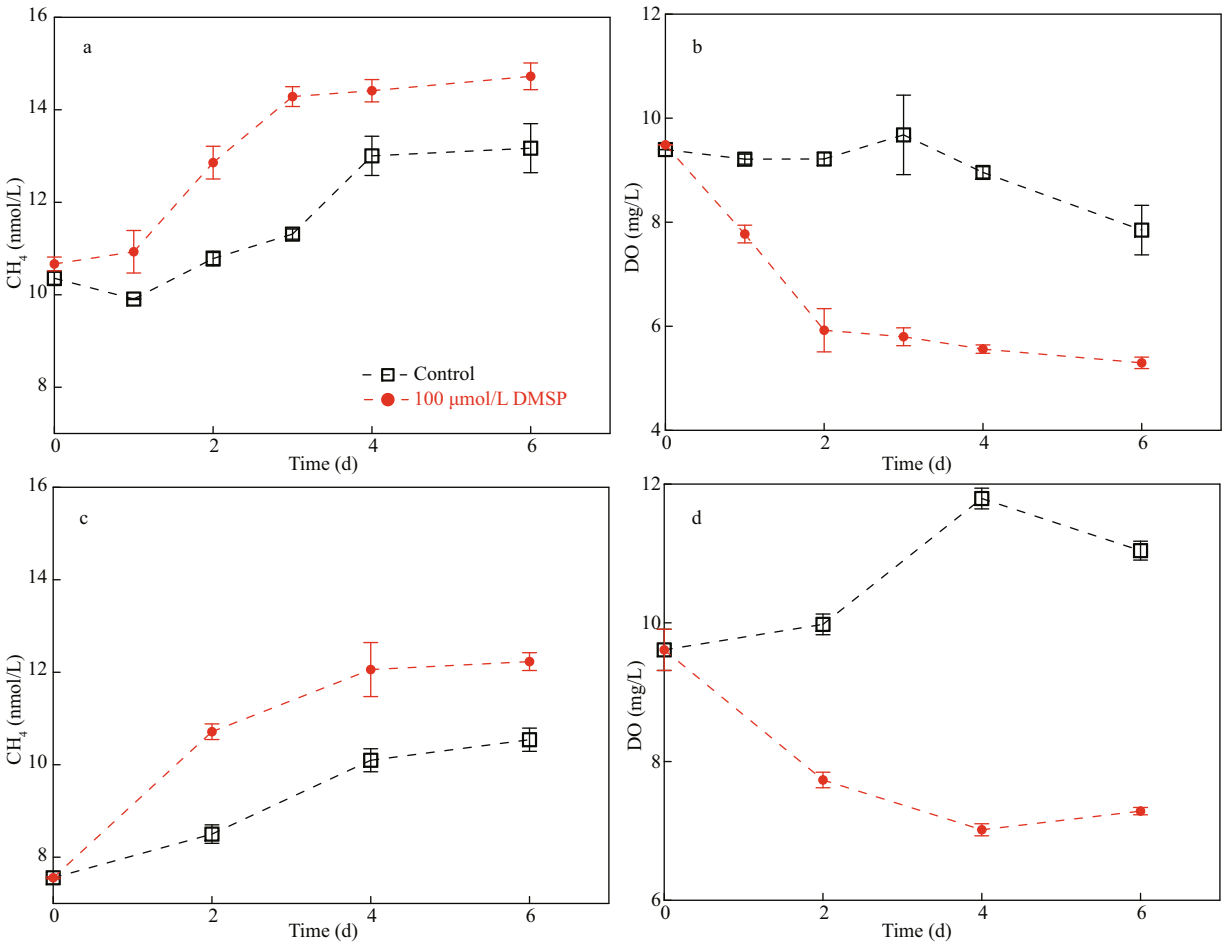

Fig.7 CH_4 production and DO consumption during DMSP-amended incubation experiments

a & b. in November 2017; c & d. in January 2018. The error bars represent one standard deviation for the triplicate bottles.

in our experiments, as reflected in the insignificant difference between the rates under N-rich treatment (5<N:P<16) and N-starved treatment (N:P<1) (Fig.8a, ANOVA, P=0.65; Supplementary Fig.S1, ANOVA, P=0.89), suggesting that N-stressed conditions may not stimulate the transformation of DMSP to CH_4 in the coastal waters. In the third experiment (seawater incubation with direct addition of DMS, see Section 2.4) CH_4 production was observed in both the positive control (amended with C+N+P) and DMS-added treatment within the first three days, but no CH_4 accumulations were observed during the last seven days in all the treatments (Fig.8c). Meanwhile, the water in the incubation bottles never became hypoxic or anoxic during this experiment (Fig.8d). The insignificant difference between the concentrations in the (C+N+P) treatment and DMS-added treatment suggested that the addition of DMS did not induce CH_4 production (ANOVA, P=0.98).

CH_4 significantly accumulated with the addition of DMSP in the first seven days compared to the control (Figs.7 & 8a), indicating that the catabolism of DMSP can contribute to the dissolved CH_4 in the presence of oxygen. The evidence for the formation of CH_4 from DMSP/DMS remains circumstantial and is mainly based on correlations between the CH_4 and DMSP/DMS concentrations (Borges et al., 2018). Two mechanisms of DMSP degradation exist in marine systems. First, the cleavage of DMSP results in DMS and acrylate, which is called dissimilation (Kiene et al., 1986; Visscher et al., 1994). Second, DMSP is demethylated to 3-mercaptopropionate (MPA), with 3-methiolpropionate (MMPA) as a possible intermediate (Kiene and Taylor, 1988); MMPA can also degrade with demethylation, yielding methanethiol (MeSH) (Fig.9) (van der Maarel and Hansen, 1997). Thus, CH_4 is known to be produced through three possible pathways: 1) Methanogenic archaea can decompose DMS to CH_4 via demethylation if the DMS concentration is high enough that sulfate-reducing bacteria do not compete with methanogens (Kiene and Taylor, 1988); 2) Microbes can utilize

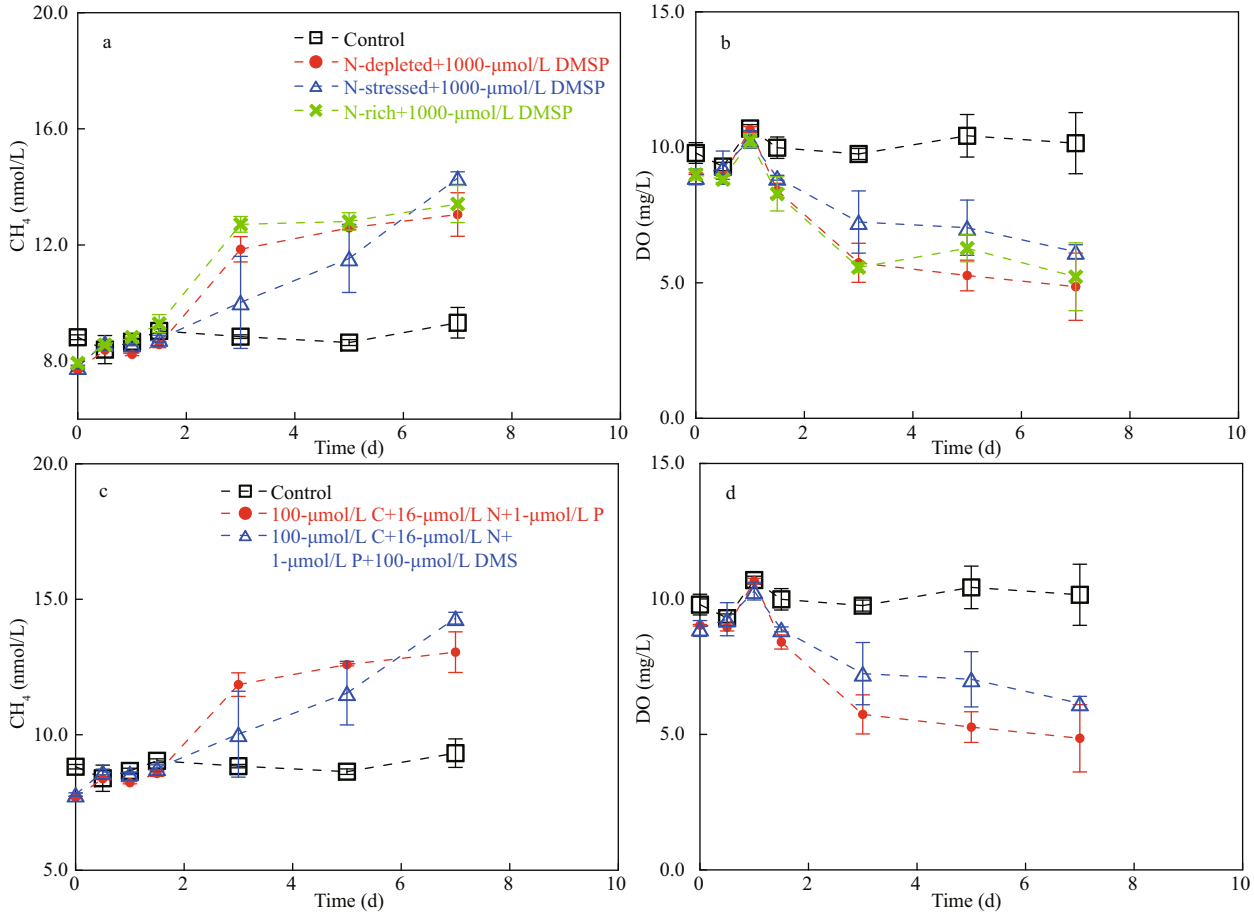

Fig.8 CH_4 and DO concentrations in surface waters incubated over time

a & b. amended with DMSP; c & d. amended with DMS. The linear regression slopes of the CH_4 concentration over time (R^2=0.33, 0.89, 0.97, and 0.86 for control, N-depleted, N-stressed, and N-rich groups, respectively, P<0.01) represent the potential CH_4 production rates (0.06, 0.89, 0.87, and 0.85 nmol/(L·d) for control, N-depleted, N-stressed, and N-rich groups, respectively) in Fig.8a. The error bars represent one standard deviation for the triplicate bottles.

MeSH (demethylation) to produce CH_4 under anoxic environments (Tallant and Krzycki, 1997); 3) Acrylate can decompose into fatty acids (such as acetate and propionate, Fig.9), which are the precursors for methanogenesis, so CH_4 can form indirectly from acrylate degradation. These possible mechanisms for the transformation of DMSP to CH_4 are thought to occur in the absence of oxygen. However, reducing conditions can form in micro-niches or inside bacterial cells (Jørgensen, 1977) despite the presence of oxygen in the ambient water. A theoretical model was recently built to explain the maintenance of anaerobic conditions for CH_4 production inside bacterial cells in association with the transformation of DMSP (Damm et al., 2015). In addition, such organisms would metabolize MeSH in cells because they must rid themselves of MeSH before it accumulates to toxic levels (Kiene et al., 1986). Thus, CH_4 may form inside cells and then be released into the oxygenated water via cell lysis (Reisch et al., 2011; Damm et al., 2015).

One concern is that the transformation efficiency

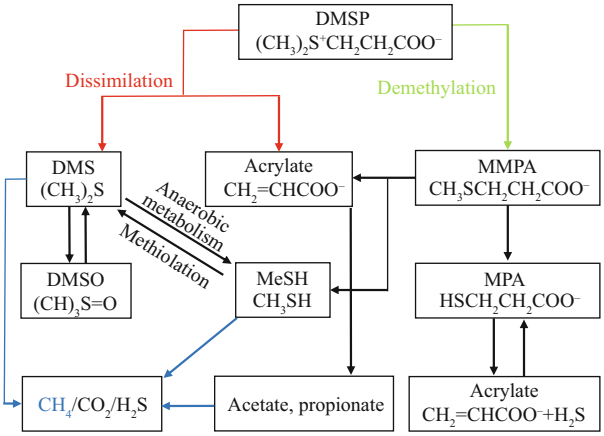

Fig.9 Schematic diagram for the conversion of DMSP and the connection with the production of CH_4

Modified from van der Maarel and Hansen (1997).

from DMSP to CH_4 in our study was low; the addition of DMSP was 100–1 000 μmol/L and the CH_4 concentration only increased by 2.0–5.0 nmol/L (Fig.8a). We suppose that this result was associated with the mechanisms of DMSP degradation. Previous

studies showed that the dissimilation pathway comprises 30% of DMSP metabolism (Kiene and Service, 1991; Kiene et al., 2000; Reisch et al., 2011; Damm et al., 2015) and only 6%–17% in surface seawater (Archer et al., 2002), which means that DMS is a minor product of DMSP metabolism. However, the first and second pathways of CH_4 formation were directly connected to the degradation of DMS (Fig.9). If limited DMS was produced from DMSP, then the yielding of CH_4 would also have been limited. Moreover, over 80% of DMS in the marine system is known to be bacterially and photochemically oxidized to dimethylsulfoxide (DMSO) (Davis et al., 1998; Nowak et al., 2001), which further reduces the conversion efficiency from DMSP to CH_4. In combination with the results of the second incubation, where CH_4 did not obviously accumulate when the treatment was directly amended with DMS (Fig.8c, ANOVA, P=0.98), we speculate that CH_4 somehow has difficulty forming directly from DMS, at least in environments such as the YS and ECS. The exact mechanism is unknown; one possibility is that CH_4-producing organisms prefer substrates other than DMS under environments where abundant carbon and sulfur sources are present (Lin et al., 2000, 2002). This observation is consistent with the negative correlations between DMS and ΔCH_4 in the ECS (Fig.4b), which means that the conversion of DMSP to CH_4 was restricted if the DMSP preferred to dissimilate to DMS. Thus, DMS accumulated in the ambient seawater but CH_4 production was limited because of the low efficiency of the DMS-to-CH_4 process. On the other hand, DMS production would be limited if the DMSP mainly degraded via demethylation (to form MPA and acrylate), whereas CH_4 would accumulate via the second and third pathways (Fig.9). Consequently, in either case, we could expect to observe positive correlations between the accumulated DMSP and ΔCH_4 and negative correlations between DMS and ΔCH_4, as we did in the field observations (Fig.4b). Another independent study that was conducted in the ECS also showed a positive correlation between DMSP and CH_4 (Zhai et al., 2019). Thus, the CH_4 in the study area may prefer to be produced via the demethylation of MeSH and/or degradation of acrylate rather than the decomposition of DMS.

Another concern is that $DMSP_d$ can be low in seawater (e.g., ~5.5 nmol/L in the YS and ECS in this study), and its contribution to the dissolved CH_4 concentration can be negligible. However, studies showed that the intracellular concentration of DMSP could reach millimolar levels (Reisch et al., 2011). Thus, the potential importance of DMSP for CH_4 production should be brought to the forefront if sulfur compounds transform in cells, as speculated above. According to the incubation experiments in the coastal waters, the DMSP-to-CH_4 production rates were estimated as an average of 0.17 nmol/(L·d) (after subtracting the rate of 0.48 nmol/(L·d) in the control) with the addition of 100-μmol/L DMSP (Fig.7a & c) and ~0.80 nmol/(L·d) with the addition of 1 000-μmol/L DMSP (Fig.8a). Our results were lower than the recently reported production rate of ~1.8 nmol/(L·d) in the central ECS with the addition of 5–10-μmol/L DMSP (Zhai et al., 2019). Damm et al. (2009) suggested that a low N:P ratio in oligotrophic areas may enhance the microbial utilization of DMSP as a C source, with CH_4 released as a by-product. However, our experiments conducted in coastal waters may weaken the effect of DMSP on CH_4 concentrations, where abundant C sources (e.g., dissolved organic carbon: 3.0 mg/L) were present for microbial assimilation (Liu et al., 2015). Thus, DMSP may be out-competed by those substrates in coastal areas because the Gibbs free energy for DMSP-dependent CH_4 production was low (-35.7 kJ/mol) (Damm et al., 2009). Consequently, even N deficiency could not trigger DMSP-dependent CH_4 production in CW (Fig.8a) because the low N:P ratio probably could not effectively stimulate the microbial utilization of DMSP in the presence of other competitive energy sources. In contrast, the experiment conducted in the oligotrophic surface seawaters of the western North Pacific (N:P<1) showed that directly addition of DMSP (10 μmol/L) induced significantly increase in CH_4 (Fig.10, ANOVA, P<0.01) and the CH_4 production rate (1.2 nmol/(L·d)) is comparable to that reported in the central ECS (Zhai et al., 2019). This suggests that the DMSP-dependent CH_4 production prefer to occur in the oligotrophic seawaters, where nitrogen is depleted.

In addition, studies showed that the $DMSP_d$ concentration in the ECS can exceed 40.0 nmol/L in summer (Yang et al., 2011) and exceed 250.0 nmol/L during blooms (Matrai and Keller, 1993), which increases the possibility of a DMSP-dependent pathway for CH_4 production in the water column. Moreover, additional CH_4 sources (such as anaerobic methanogenesis in micro-niches and the degradation of Carbon-Phosphorus/Carbon-Nitrogen bonded compounds) alongside DMSP pathways should exist

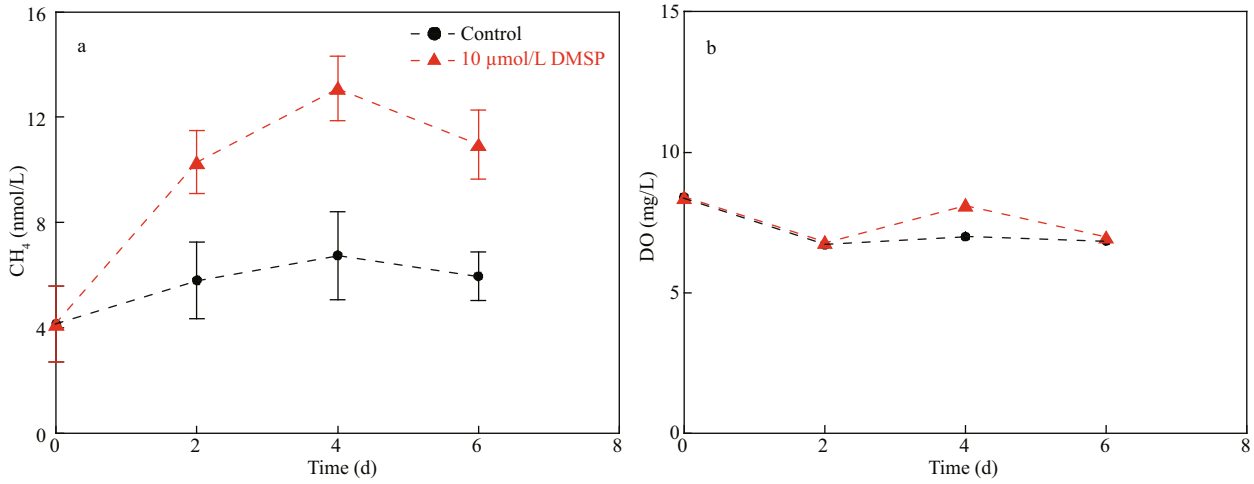

Fig.10 Incubation experiment for seawaters directly amended with DMSP in the oligotrophic Western North Pacific

a. CH_4 production; b. oxygen consumption. The final concentration of DMSP was 10 μmol/L. The error bars represent one standard deviation for the triplicate bottles.

in the oxygenated water column to maintain the loss of CH_4 into the atmosphere. Recently, CH_4 production from MPn was attributed to microbial activity in P-starved oceanic areas (Karl et al., 2008; Metcalf et al., 2012; Repeta et al., 2016). Our recent experiments in the YS also indicated the possibility of a Carbon-Phosphorus cleavage pathway for the enrichment of CH_4 in oxic water (Ye et al., 2020). Hence, the CH_4 dynamics in the YS and ECS are complicated, and CH_4 production in well-oxygenated water may be attributed to several mechanisms. According to our field observations and incubation experiments, the Carbon-Sulfur cleavage pathway for CH_4 production in well-oxygenated water is a potential mechanism for the production of excess CH_4 in the western North Pacific. Although the exact molecular mechanism is unclear and no direct evidence exists of carbon transfer from DMSP to CH_4, the implications for the biogeochemical cycling of carbon and sulfur in the marine system is essential to future work, especially when considering the effect of CH_4 and DMS on global warming and atmospheric chemistry.

4 CONCLUSION

The CH_4 concentrations in the ECS and YS showed great variations among different water masses, which profoundly affected the CH_4 distribution. In spring, the vertical profiles of CH_4 were homogenous in the YS but varied greatly in the ECS because of the latter's more complicated hydrological conditions. The surface and subsurface waters are oversaturated in CH_4 indicated that the YS and ECS are the net sources of atmospheric CH_4 in spring. A box model was used to evaluate the CH_4 dynamics in the ECS. The results suggested that the coastal water plays an important role in distributing CH_4 among the near-shore areas, while it was a minor source (0.01%) for CH_4 in the continental shelf because of the low water discharge. Over 95% CH_4 was considered to be produced and consumed in the shelf water, subsequently with 2.2% CH_4 diffused to the atmosphere, suggesting ECS is a hotspot for CH_4 dynamics. Further incubation experiments were carried out to figure out the source of this hotspot. Results show that DMSP can be a potential CH_4 precursor in oxygenated coastal water and DMSP-dependent CH_4 production has potential to be enhanced in oligotrophic areas.

This study demonstrates that the in-situ production could be a major source of dissolved CH_4 in the marginal seas of China and its correlation with cleaving of Carbon-Sulfur bonded compounds (such as DMSP and MeSH) may have further implications for carbon and sulfur biogeochemical processes in the western Pacific. Further work is required to confirm the intrinsic connections between methylated sulfur compounds and CH_4, presumably by molecular-biology techniques.

5 DATA AVAILABILITY STATEMENT

All data included in this study are available upon request by contact with the corresponding author.

6 ACKNOWLEDGMENT

The authors wish to thank the crews of the R/V *Dong Fang Hong 2* and colleagues from the Laboratory of Marine Biogeochemistry at the Ocean

University of China for their assistance with the collection of field samples. We also thank Haibing DING from the Ocean University of China for providing CH_4 oxidation data.

7 CONFLICT OF INTEREST

The authors declare that they have no conflict of interest.

References

Araujo J, Pratihary A, Naik R, Naik H, Naqvi S W A. 2018. Benthic fluxes of methane along the salinity gradient of a tropical monsoonal estuary: implications for CH_4 supersaturation and emission. *Marine Chemistry*, **202**: 73-85, https://doi.org/10.1016/j.marchem.2018.03.008.

Archer S D, Gilbert F J, Nightingale P D, Zubkov M V, Taylor A H, Smith G C, Burkill P H. 2002. Transformation of dimethylsulphoniopropionate to dimethyl sulphide during summer in the North Sea with an examination of key processes via a modelling approach. *Deep Sea Research Part II*: *Topical Studies in Oceanography*, **49**(15): 3067-3101, https://doi.org/10.1016/S0967-0645(02)00072-3.

Bange H W, Bartell U H, Rapsomanikis S, Andreae M O. 1994. Methane in the Baltic and North Seas and a reassessment of the marine emissions of methane. *Global Biogeochemical Cycles*, **8**(4): 465-480, https://doi.org/10.1029/94GB02181.

Bange H W, Bergmann K, Hansen H P, Kock A, Koppe R, Malien F, Ostrau C. 2010. Dissolved methane during hypoxic events at the Boknis Eck time series station (Eckernförde Bay, SW Baltic Sea). *Biogeosciences*, **7**(4): 1279-1284, https://doi.org/10.5194/bg-7-1279-2010.

Borges A V, Speeckaert G, Champenois W, Scranton M I, Gypens N. 2018. Productivity and temperature as drivers of seasonal and spatial variations of dissolved methane in the Southern Bight of the North Sea. *Ecosystems*, **21**(4): 583-599, https://doi.org/10.1007/s10021-017-0171-7.

Bryan J R, Rlley J P, Williams P J L. 1976. A winkler procedure for making precise measurements of oxygen concentration for productivity and related studies. *Journal of Experimental Marine Biology and Ecology*, **21**(3): 191-197, https://doi.org/10.1016/0022-0981(76)90114-3.

Bussmann I, Hackbusch S, Schaal P, Wichels A. 2017. Methane distribution and oxidation around the Lena Delta in summer 2013. *Biogeosciences*, **14**(21): 4985-5002, https://doi.org/10.5194/bg-14-4985-2017.

Chen C T A, Wang S L. 1999. Carbon, alkalinity and nutrient budgets on the East China Sea continental shelf. *Journal of Geophysical Research*: *Oceans*, **104**(C9): 20675-20686, https://doi.org/10.1029/1999jc900055.

Damm E, Helmke E, Thoms S, Schauer U, Nöthig E, Bakker K, Kiene R P. 2009. Methane production in aerobic oligotrophic surface water in the central Arctic Ocean. *Biogeosciences*, **6**: 10355-10379, https://doi.org/10.5194/bgd-6-10355-2009.

Damm E, Kiene R P, Schwarz J, Falck E, Dieckmann G. 2008. Methane cycling in Arctic shelf water and its relationship with phytoplankton biomass and DMSP. *Marine Chemistry*, **109**(1-2): 45-59, https://doi.org/10.1016/j.marchem.2007.12.003.

Damm E, Thoms S, Beszczynska-Möller A, Nöthig E M, Kattner G. 2015. Methane excess production in oxygen-rich polar water and a model of cellular conditions for this paradox. *Polar Science*, **9**(3): 327-334, https://doi.org/10.1016/j.polar.2015.05.001.

Davis D, Chen G, Kasibhatla P, Jefferson A, Tanner D, Eisele F, Lenschow D, Neff W, Berresheim H. 1998. DMS oxidation in the Antarctic marine boundary layer: comparison of model simulations and held observations of DMS, DMSO, $DMSO_2$, H_2SO_4(g), MSA(g), and MSA(p). *Journal of Geophysical Research*: *Atmospheres*, **103**(D1): 1657-1678, https://doi.org/10.1029/97JD03452.

de Angelis M A, Lee C. 1994. Methane production during zooplankton grazing on marine phytoplankton. *Limnology and Oceanography*, **39**(6): 1298-1308, https://doi.org/10.4319/lo.1994.39.6.1298.

Di P F, Feng D, Tao J, Chen D F. 2020. Using time-series videos to quantify methane bubbles flux from natural cold seeps in the South China Sea. *Minerals*, **10**(3): 216, https://doi.org/10.3390/min10030216.

Ferrón S, Alonso-Pérez F, Ortega T, Forja J M. 2009. Benthic respiration on the northeastern shelf of the Gulf of Cádiz (SW Iberian Peninsula). *Marine Ecology Progress Series*, **392**: 69-80, https://doi.org/10.3354/meps08240.

Florez-Leiva L, Damm E, Farías L. 2013. Methane production induced by dimethylsulfide in surface water of an upwelling ecosystem. *Progress in Oceanography*, **112-113**: 38-48, https://doi.org/10.1016/j.pocean.2013.03.005.

Grossart H P, Frindte K, Dziallas C, Eckert W, Tang K W. 2011. Microbial methane production in oxygenated water column of an oligotrophic lake. *Proceedings of the National Academy of Sciences of the United States of America*, **108**(49): 19657-19661, https://doi.org/10.1073/pnas.1110716108.

Guan B X, Fang G H. 2006. Winter counter-wind currents off the southeastern China coast: a review. *Journal of Oceanography*, **62**(1): 1-24, https://doi.org/10.1007/s10872-006-0028-8.

Günthel M, Donis D, Kirillin G, Ionescu D, Bizic M, McGinnis D F, Grossart H P, Tang K W. 2019. Contribution of oxic methane production to surface methane emission in lakes and its global importance. *Nature Communications*, **10**(1): 5497, https://doi.org/10.1038/s41467-019-13320-0.

Hickox R, Belkin I, Cornillon P, Shan Z Q. 2000. Climatology and seasonal variability of ocean fronts in the East China, Yellow and Bohai seas from satellite SST data. *Geophysical Research Letters*, **27**(18): 2945-2948, https://doi.org/10.1029/1999GL011223.

IPCC. 2013. Climate Change 2013: The Physical Science Basis. Cambridge University Press, New York.

Jackson J E. 1991. A User's Guide to Principal Components. John Wiley & Sons, New York.

Jiang S, Zhang J, Zhang R F, Xue Y, Zheng W. 2018. Dissolved lead in the East China Sea with implications for impacts of marginal seas on the open ocean through cross-shelf exchange. *Journal of Geophysical Research*: *Oceans*, **123**(8): 6004-6018, https://doi.org/10.1029/2018JC013955.

Jin J, Liu S M, Ren J L, Liu C G, Zhang J, Zhang G L, Huang D J. 2013. Nutrient dynamics and coupling with phytoplankton species composition during the spring blooms in the Yellow Sea. *Deep Sea Research Part II*: *Topical Studies in Oceanography*, **97**: 16-32, https://doi.org/10.1016/j.dsr2.2013.05.002.

Jørgensen B B, Weber A, Zopfi J. 2001. Sulfate reduction and anaerobic methane oxidation in Black Sea sediments. *Deep Sea Research Part I*: *Oceanographic Research Papers*, **48**(9): 2097-2120, https://doi.org/10.1016/S0967-0637(01)00007-3.

Jørgensen B B. 1977. Bacterial sulfate reduction within reduced microniches of oxidized marine sediments. *Marine Biology*, **41**(1): 7-17, https://doi.org/doi:10.1007/bf00390576.

Judd A G. 2004. Natural seabed gas seeps as sources of atmospheric methane. *Environmental Geology*, **46**(8): 988-996, https://doi.org/10.1007/s00254-004-1083-3.

Karl D M, Beversdorf L, Björkman K M, Church M J, Martinez A, Delong E F. 2008. Aerobic production of methane in the sea. *Nature Geoscience*, **1**(7): 473-478, https://doi.org/10.1038/ngeo234.

Karl D M, Tilbrook B D. 1994. Production and transport of methane in oceanic particulate organic matter. *Nature* **368**(6473): 732-734, https://doi.org/10.1038/368732a0.

Kiene R P, Linn L J, Bruton J A. 2000. New and important roles for DMSP in marine microbial communities. *Journal of Sea Research*, **43**(3-4): 209-224, https://doi.org/10.1016/S1385-1101(00)00023-X.

Kiene R P, Oremland R S, Catena A, Miller L G, Capone D G. 1986. Metabolism of reduced methylated sulfur compounds in anaerobic sediments and by a pure culture of an estuarine methanogen. *Applied and Environmental Microbiology*, **52**(5): 1037-1045, https://doi.org/10.1128/AEM.52.5.1037-1045.1986.

Kiene R P, Service S K. 1991. Decomposition of dissolved DMSP and DMS in estuarine waters: dependence on temperature and substrate concentration. *Marine Ecology Progress Series*, **76**: 1-11, https://doi.org/10.3354/meps076001.

Kiene R P, Taylor B F. 1988. Demethylation of dimethylsulfoniopropionate and production of thiols in anoxic marine sediments. *Applied and Environmental Microbiology*, **54**(9): 2208-2212, https://doi.org/10.1002/bit.260320617.

Li C X, Yang G P, Wang B D, Xu Z J. 2016. Vernal distribution and turnover of dimethylsulfide (DMS) in the surface water of the Yellow Sea. *Journal of Geophysical Research*: *Oceans*, **121**(10): 7495-7516, https://doi.org/10.1002/2016JC011901.

Li F. 1989. Distinction, discrimination and analysis of water masses in the Yellow Sea and East China Sea areas in spring. *Journal of Ocean University of Qingdao*, **19**(1): 22-34, http://doi.org/10.16441/j.cnki.hdxb.1989.s1.007. (in Chinese with English abstract)

Li W, Wang Y H, Wang J N, Wei H. 2012. Distributions of water masses and hydrographic structures in the Yellow Sea and East China Sea in spring and summer 2011. *Oceanologia et Limnologia Sinica*, **43**(3): 615-623. (in Chinese with English abstract)

Lin S, Hsieh I J, Huang K M, Wang C H. 2002. Influence of the Yangtze River and grain size on the spatial variations of heavy metals and organic carbon in the East China Sea continental shelf sediments. *Chemical Geology*, **182**(2-4): 377-394, https://doi.org/10.1016/s0009-2541(01)00331-x.

Lin S, Huang K M, Chen S K. 2000. Organic carbon deposition and its control on iron sulfide formation of the southern East China Sea continental shelf sediments. *Continental Shelf Research*, **20**(4-5): 619-635, https://doi.org/10.1016/S0278-4343(99)00088-6.

Liu J, Yu Z G, Zang J Y, Sun T, Zhao C Y, Ran X B. 2015. Distribution and budget of organic carbon in the Bohai and Yellow Seas. *Advances in Earth Science*, **30**(5): 564-578, https://doi.org/10.11867/j.issn.1001-8166.2015.05.564. (in Chinese with English abstract)

Luong L D, Shakirov R B, Hoang N, Shinjo R, Obzhirov A, Syrbu N, Shakirova M. 2019. Features in REE and methane anomalies distribution in the East China Sea water column: a comparison with the South China Sea. *Water Resources*, **46**: 807-816, https://doi.org/10.1134/S0097807819050142.

Luong L D, Shinjo R, Hoang N, Shakirov R B, Syrbu N. 2018. Spatial variations in dissolved rare earth element concentrations in the East China Sea water column. *Marine Chemistry*, **205**: 1-15, https://doi.org/10.1016/j.marchem.2018.07.004.

Martínez A, Ventouras L A, Wilson S T, Karl D M, DeLong E F. 2013. Metatranscriptomic and functional metagenomic analysis of methylphosphonate utilization by marine bacteria. *Frontiers in Microbiology*, **4**: 340, https://doi.org/10.3389/fmicb.2013.00340.

Matrai P A, Keller M D. 1993. Dimethylsulfide in a large-scale coccolithophore bloom in the Gulf of Maine. *Continental Shelf Research*, **13**(8-9): 831-843, https://doi.org/10.1016/0278-4343(93)90012-M.

Matsuno T, Lee J S, Yanao S. 2009. The Kuroshio exchange with the South and East China Seas. *Ocean Science*, **5**(3): 303-312, https://doi.org/10.5194/os-5-303-2009.

Metcalf W W, Griffin B M, Cicchillo R M, Gao J T, Janga S C, Cooke H A, Circello B T, Evans B S, Martens-Habbena W, Stahl D A, van der Donk W A. 2012. Synthesis of methylphosphonic acid by marine microbes: a source for methane in the aerobic ocean. *Science*, **337**(6098): 1104-1107, https://doi.org/10.1126/science.1219875.

Nowak J B, Davis D D, Chen G, Eisele F L, Mauldin R L, Tanner D J, Cantrell C, Kosciuch E, Bandy A, Thornton

D, Clarke A. 2001. Airborne observations of DMSO, DMS, and OH at marine tropical latitudes. *Geophysical Research Letters*, **28**(11): 2201-2204, https://doi.org/10.1029/2000GL012297.

Osudar R, Matoušů A, Alawi M, Wagner D, Bussmann I. 2015. Environmental factors affecting methane distribution and bacterial methane oxidation in the German Bight (North Sea). *Estuarine*, *Coastal and Shelf Science*, **160**: 10-21, https://doi.org/10.1016/j.ecss.2015.03.028.

Qi J F, Yin B S, Zhang Q L, Yang D Z, Xu Z H. 2014. Analysis of seasonal variation of water masses in East China Sea. *Chinese Journal of Oceanology and Limnology*, **32**(4): 958-971, https://doi.org/10.1007/s00343-014-3269-1.

Rao G D, Sarma V V S S. 2016. Variability in concentrations and fluxes of methane in the Indian estuaries. *Estuaries and Coasts*, **39**(6): 1639-1650, https://doi.org/10.1007/s12237-016-0112-2.

Reisch C R, Moran M A, Whitman W B. 2011. Bacterial catabolism of dimethylsulfoniopropionate (DMSP). *Frontiers in Microbiology*, **2**: 172, https://doi.org/10.3389/fmicb.2011.00172.

Repeta D J, Ferrón S, Sosa O A, Johnson C G, Repeta L D, Acker M, DeLong E F, Karl D M. 2016. Marine methane paradox explained by bacterial degradation of dissolved organic matter. *Nature Geoscience*, **9**(12): 884-887, https://doi.org/10.1038/ngeo2837.

Rogener M K, Bracco A, Hunter K S, Saxton M A, Joye S B. 2018. Long-term impact of the Deepwater Horizon oil well blowout on methane oxidation dynamics in the northern Gulf of Mexico. *Elementa*: *Science of the Anthropocene*, **6**: 73, https://doi.org/10.1525/elementa.332.

Rogener M K, Sipler R E, Hunter K S, Bronk D A, Joye S B. 2019. Pelagic methane oxidation in the northern Chukchi Sea. *Limnology and Oceanography*, **65**(1): 96-110, https://doi.org/10.1002/lno.11254.

Sakai H, Gamo T, Kim E S, Tsutsumi M, Tanaka T, Ishibashi J, Wakita H, Yamano M, Oomori T. 1990. Venting of carbon dioxide-rich fluid and hydrate formation in Mid-Okinawa trough Backarc basin. *Science*, **248**(4959): 1093-1096, https://doi.org/10.1126/science.248.4959.1093.

Saunois M, Stavert A R, Poulter B, Bousquet P, Bousquet P, Canadell J G, Jackson R B, Raymond P A, Dlugokencky E J, Houweling S, Patra P K, Ciais P, Arora V K, Bastviken D, Bergamaschi P, Blake D R, Brailsford G, Bruhwiler L, Carlson K M, Carrol M, Castaldi S, Chandra N, Crevoisier C, Crill P M, Covey K, Curry C L, Etiope G, Frankenberg C, Gedney N, Hegglin M I, Höglund-Isaksson L, Hugelius G, Ishizawa M, Ito A, Janssens-Maenhout G, Jensen K M, Joos F, Kleinen T, Krummel P B, Langenfelds R L, Laruelle G G, Liu L, Machida T, Maksyutov S, McDonald K C, McNorton J, Miller P A, Melton J R, Morino I, Müller J, Murguia-Flores F, Naik V, Niwa Y, Noce S, O'Doherty S, Parker R J, Peng C H, Peng S S, Peters G P, Prigent C, Prinn R, Ramonet M, Regnier P, Riley W J, Rosentreter J A, Segers A, Simpson I J, Shi H, Smith S J, Steele L P, Thornton B F, Tian H, Tohjima Y, Tubiello F N, Tsuruta A, Viovy N, Voulgarakis A, Weber T S, van Weele M, van der Werf G R, Weiss R F, Worthy D, Wunch D, Yin Y, Yoshida Y, Zhang W X, Zhang Z, Zhao Y H, Zheng B, Zhu Q, Zhu Q, Zhuang Q L. 2020. The global methane budget 2000-2017. *Earth System Science Data*, **12**(3): 1561-1623, https://doi.org/10.5194/essd-12-1561-2020.

Sawicka J E, Brüchert V. 2017. Annual variability and regulation of methane and sulfate fluxes in Baltic Sea estuarine sediments. *Biogeosciences*, **14**(2): 325-339, https://doi.org/10.5194/bg-14-325-2017.

Schmale O, Wäge J, Mohrholz V, Wasmund N, Gräwe U, Rehder G, Labrenz M, Loick-Wilde N. 2018. The contribution of zooplankton to methane supersaturation in the oxygenated upper waters of the central Baltic Sea. *Limnology and Oceanography*, **63**(1): 412-430, https://doi.org/10.1002/lno.10640.

Shakhova N, Semiletov I, Leifer I, Sergienko V, Salyuk A, Kosmach D, Chernykh D, Stubbs C, Nicolsky D, Tumskoy V, Gustafsson Ö. 2014. Ebullition and storm-induced methane release from the East Siberian Arctic Shelf. *Nature Geoscience*, **7**(1): 64-70, https://doi.org/10.1038/ngeo2007.

Sosa O A, Burrell T J, Wilson S T, Foreman R K, Karl D M, Repeta D J. 2020. Phosphonate cycling supports methane and ethylene supersaturation in the phosphate-depleted western North Atlantic Ocean. *Limnology and Oceanography*, **65**(10): 2443-2459, https://doi.org/10.1002/lno.11463.

Sosa O A, Repeta D J, Ferrón S, Bryant J A, Mende D R, Karl D M, DeLong E F. 2017. Isolation and characterization of bacteria that degrade phosphonates in marine dissolved organic matter. *Frontiers in Microbiology*, **8**: 1786, https://doi.org/10.3389/fmicb.2017.01786.

Stawiarski B, Otto S, Thiel V, Gräwe U, Loick-Wilde N, Wittenborn A K, Schloemer S, Wäge, J, Rehder G, Labrenz M, Wasmund N, Schmale O. 2019. Controls on zooplankton methane production in the central Baltic Sea. *Biogeosciences*, **16**(1): 1-16, https://doi.org/10.5194/bg-16-1-2019.

Su J L. 1998. Circulation Dynamics of the China Seas: North of 18°N. *In*: The Sea: Vol. 11. The Global Coastal Ocean: Reginal Studies and Synthesis. John Wiley & Sons Inc., New York. p.483-505.

Sun M S, Zhang G L, Ma X, Cao X P, Mao X Y, Li J, Ye W W, Liu S M. 2018. Dissolved methane in the East China Sea: distribution, seasonal variation and emission. *Marine Chemistry*, **202**: 12-26, https://doi.org/10.1016/j.marchem.2018.03.001.

Tallant T C, Krzycki J A. 1997. Methylthiol: coenzyme M methyltransferase from *Methanosarcina barkeri*, an enzyme of methanogenesis from dimethylsulfide and methylmercaptopropionate. *Journal of Bacteriology*, **179**(22): 6902-6911, https://doi.org/10.1128/jb.179.22.6902-6911.1997.

Tang Y X, Lie H J, Cho C H, Lee J H. 1997. The hydrographic condition in the northeastern East China Sea in summer. *Journal of Oceanography of Huanghai & Bohai Seas*,

15(1): 8-19. (in Chinese with English abstract)

Teikari J E, Fewer D P, Shrestha R, Hou S W, Leikoski N, Mäkelä M, Simojoki A, Hess W R, Sivonen K. 2018. Strains of the toxic and bloom-forming *Nodularia spumigena* (cyanobacteria) can degrade methylphosphonate and release methane. *The ISME Journal*, **12**(6): 1619-1630, https://doi.org/10.1038/s41396-018-0056-6.

Treude T, Niggemann J, Kallmeyer J, Wintersteller P, Schubert C J, Boetius A, Jørgensen B B. 2005. Anaerobic oxidation of methane and sulfate reduction along the Chilean continental margin. *Geochimica et Cosmochimica Acta*, **69**(11): 2767-2779, https://doi.org/10.1016/j.gca.2005.01.002.

Valentine D L. 2002. Biogeochemistry and microbial ecology of methane oxidation in anoxic environments: a review. *Antonie van Leeuwenhoek*, **81**(1): 271-282, https://doi.org/10.1023/A:1020587206351.

van der Maarel M J E C, Hansen T A. 1997. Dimethylsulfoniopropionate in anoxic intertidal sediments: a precursor of methanogenesis via dimethyl sulfide, methanethiol, and methiolpropionate. *Marine Geology*, **137**(1-2): 5-12, https://doi.org/10.1016/S0025-3227(96)00074-6.

Visscher P T, Kiene R P, Taylor B F. 1994. Demethylation and cleavage of dimethylsulfoniopropionate in marine intertidal sediments. *FEMS Microbiology Ecology*, **14**(2): 179-189, https://doi.org/10.1111/j.1574-6941.1994.tb00104.x.

Wäge J, Schmale O, Labrenz M. 2020. Quantification of methanogenic Archaea within Baltic Sea copepod faecal pellets. *Marine Biology*, **167**(10): 153, https://doi.org/10.1007/s00227-020-03759-x.

Wang Y C, Guo X Y, Zhao L, Zhang J. 2019. Seasonal variations in nutrients and biogenic particles in the upper and lower layers of East China Sea Shelf and their export to adjacent seas. *Progress in Oceanography*, **176**: 102138, https://doi.org/10.1016/j.pocean.2019.102138.

Weber T, Wiseman N A, Kock A. 2019. Global ocean methane emissions dominated by shallow coastal waters. *Nature Communication*, **10**(1): 4584, https://doi.org/10.1038/s41467-019-12541-7.

Webster R. 2009. Statistics to support soil research and their presentation. *European Journal of Soil Science*, **52**(2): 331-340, https://doi.org/10.1046/j.1365-2389.2001.00383.x.

Yamamoto H, Fujimori T, Sato H, Ishikawa G, Kami K, Ohashi Y. 2014. Statistical hypothesis testing of factor loading in principal component analysis and its application to metabolite set enrichment analysis. *BMC Bioinformatics* **15**(1): 1-9, https://doi.org/10.1186/1471-2105-15-51.

Yang D Z, Yin B S, Chai F, Feng X R, Xue H J, Gao G D, Yu F. 2018. The onshore intrusion of Kuroshio subsurface water from February to July and a mechanism for the intrusion variation. *Progress in Oceanography*, **167**: 97-115, https://doi.org/10.1016/j.pocean.2018.08.004.

Yang G P, Jing W W, Kang Z Q, Zhang H H, Song G S. 2008. Spatial variations of dimethylsulfide and dimethylsulfoniopropionate in the surface microlayer and in the subsurface waters of the South China Sea during springtime. *Marine Environmental Research*, **65**(1): 85-97, https://doi.org/10.1016/j.marenvres.2007.09.002.

Yang G P, Zhang H H, Zhou L M, Yang J. 2011. Temporal and spatial variations of dimethylsulfide (DMS) and dimethylsulfoniopropionate (DMSP) in the East China Sea and the Yellow Sea. *Continental Shelf Research*, **31**(13): 1325-1335, https://doi.org/10.1016/j.csr.2011.05.001.

Yang J, Zhang G L, Zheng L X, Zhang F, Zhao J. 2010. Seasonal variation of fluxes and distributions of dissolved methane in the North Yellow Sea. *Continental Shelf Research*, **30**(2): 187-192, https://doi.org/10.1016/j.csr.2009.10.016.

Ye W W, Wang X L, Zhang X H, Zhang G L. 2020. Methane production in oxic seawater of the western North Pacific and its marginal seas. *Limnology and Oceanography*, **65**(10): 2352-2365, https://doi.org/10.1002/lno.11457.

Ye W W, Zhang G L, Zheng W J, Zhang H H, Wu Y. 2019. Methane distributions and sea-to-air fluxes in the Pearl River Estuary and the northern South China Sea. *Deep Sea Research Part II*: *Topical Studies in Oceanography*, **167**: 34-45, https://doi.org/10.1016/j.dsr2.2019.06.016.

Ye W W, Zhang G L, Zhu Z Y, Huang D J, Han Y, Wang L, Sun M S. 2016. Methane distribution and sea-to-air flux in the East China Sea during the summer of 2013: impact of hypoxia. *Deep Sea Research Part II*: *Topical Studies in Oceanography*, **124**: 74-83, https://doi.org/10.1016/j.dsr2.2015.01.008.

Zhai X, Li J L, Zhang H H, Tan D D, Yang G P. 2019. Spatial distribution and biogeochemical cycling of dimethylated sulfur compounds and methane in the East China Sea during spring. *Journal of Geophysical Research*: *Oceans*, **124**(2): 1074-1090, https://doi.org/10.1029/2018JC014488.

Zhang G L, Zhang J, Kang Y B, Liu S M. 2004. Distributions and fluxes of methane in the East China Sea and the Yellow Sea in spring. *Journal of Geophysical Research*: *Oceans*, **109**(C7): C07011, https://doi.org/10.1029/2004JC002268.

Zhang G L, Zhang J, Liu S M, Ren J L, Xu J, Zhang F. 2008a. Methane in the Changjiang (Yangtze River) Estuary and its adjacent marine area: riverine input, sediment release and atmospheric fluxes. *Biogeochemistry*, **91**(1): 71-84, https://doi.org/10.1007/s10533-008-9259-7.

Zhang G L, Zhang J, Ren J L, Li J B, Liu S M. 2008b. Distributions and sea-to-air fluxes of methane and nitrous oxide in the North East China Sea in summer. *Marine Chemistry*, **110**(1-2): 42-55, https://doi.org/10.1016/j.marchem.2008.02.005.

Zhang J, Liu Q, Bai L L, Matsuno T. 2018. Water mass analysis and contribution estimation using heavy rare earth elements: significance of Kuroshio intermediate water to Central East China Sea shelf water. *Marine Chemistry*, **204**: 172-180, https://doi.org/10.1016/j.marchem.2018.07.011.

Zhang J, Liu S M, Ren J L, Wu Y, Zhang G L. 2007. Nutrient gradients from the eutrophic Changjiang (Yangtze River)

Estuary to the oligotrophic Kuroshio waters and re-evaluation of budgets for the East China Sea Shelf. *Progress in Oceanography*, **74**(4): 449-478, https://doi.org/10.1016/j.pocean.2007.04.019.

Zhao B, Yao P, Bianchi T S, Arellano A R, Wang X C, Yang J B, Su R G, Wang J P, Xu Y H, Huang X Y, Chen L, Ye J, Yu Z G. 2018. The remineralization of sedimentary organic carbon in different sedimentary regimes of the Yellow and East China Seas. *Chemical Geology*, **495**: 104-117, https://doi.org/10.1016/j.chemgeo.2018.08.012.

Zhou P, Song X X, Yuan Y Q, Wang W T, Chi L B, Cao X H, Yu Z M. 2018. Intrusion of the Kuroshio Subsurface Water in the southern East China Sea and its variation in 2014 and 2015 traced by dissolved inorganic iodine species. *Progress in Oceanography*, **165**: 287-298, https://doi.org/10.1016/j.pocean.2018.06.011.

Zindler C, Bracher A, Marandino C A, Taylor B, Torrecilla E, Kock A, Bange H W. 2013. Sulphur compounds, methane, and phytoplankton: interactions along a north-south transit in the western Pacific Ocean. *Biogeosciences*, **10**(5): 3297-3311, https://doi.org/10.5194/bg-10-3297-2013.

Electronic supplementary material

Supplementary material (Supplementary Tables S1–S4 and Fig.S1) is available in the online version of this article at https://doi.org/10.1007/s00343-021-1010-4.